

Finite Element Modeling for Electrical Energy Applications
Lecture Notes for ET4375

Dr. D. Lahaye and Helping Friends

February 16, 2012

Chapter 1

Introduction

In this chapter we aim at

- describing the different stages in a finite element method (FEM) modeling procedure;
- give an example of FEM is applied in the modeling of an electrical energy application.

Extension of these notes

- animations
- visualization using COVISE
- visualization using

1.1 Stages in a FEM Modeling Procedure

Figure 1.1 shows five different stages in the finite element method (FEM) modeling of the mechanical deformation of a microchip caused by the Ohmic heat generated by an electrical current. The following five stages can be distinguished:

- in **Stage 1** a geometry model of the device under consideration is built. For this purpose a computer aided design (CAD) software package is typically used;
- in **Stage 2** the governing physical processes are described in terms of appropriate partial differential equations supplied with initial and boundary conditions. In the modeling of electrical energy applications, the Maxwell equations for the electric and magnetic field will play a central role;
- in **Stage 3** the geometry is subdivided into small entities called elements. Different types of mesh generation and mesh refinement techniques exist.
- in **Stage 4** the governing partial differential equations are discretized in space and time and the resulting (non-)linear systems of equations are solved.
- in **Stage 5** the solution of the partial differential equations and derived quantities are visualized on the mesh employed for discretization in space and time.

These five stages are typical in any FEM modeling procedure. Although the other stages are not trivial and object of active research, this course mainly focusses on **Stage 2** and **Stage 4**.

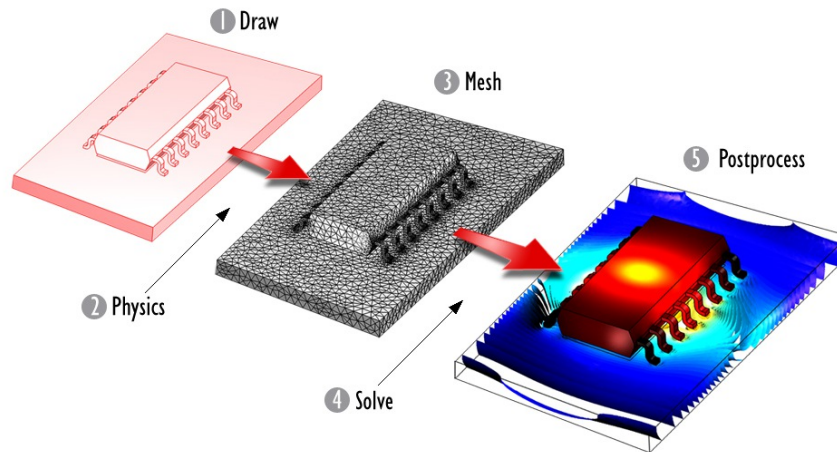
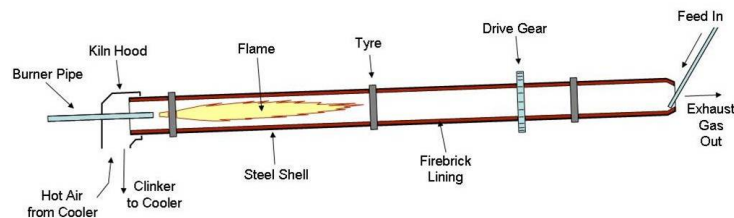


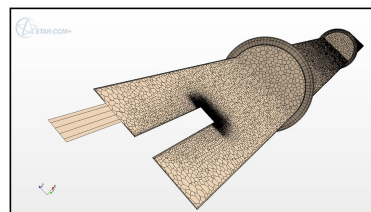
Figure 1.1: Stages in a FEM Modeling Procedure.

1.2 Motivating Examples

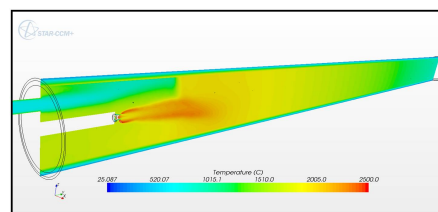
Industrial Furnace The simulation of flows through an enclosed surface is an often reoccurring problem in computational fluid dynamics. In Figure 1.2 a study case of the simulation of the flow and temperature profile inside an industrial furnace is presented.



(a) Schematic representation of an industrial furnace



(b) Mesh employed



(c) Simulated temperature profile.

Figure 1.2: Numerical simulation of industrial furnaces.

Fault current limiters Fault current limiters are expected to play an important role in the protection of future power grids. They are capable of preventing fault currents from reaching too high levels and, therefore enhance the life time expectancy all power system components. Figure 1.3 shows two examples of fault-current limiters along with some finite element simulation results.

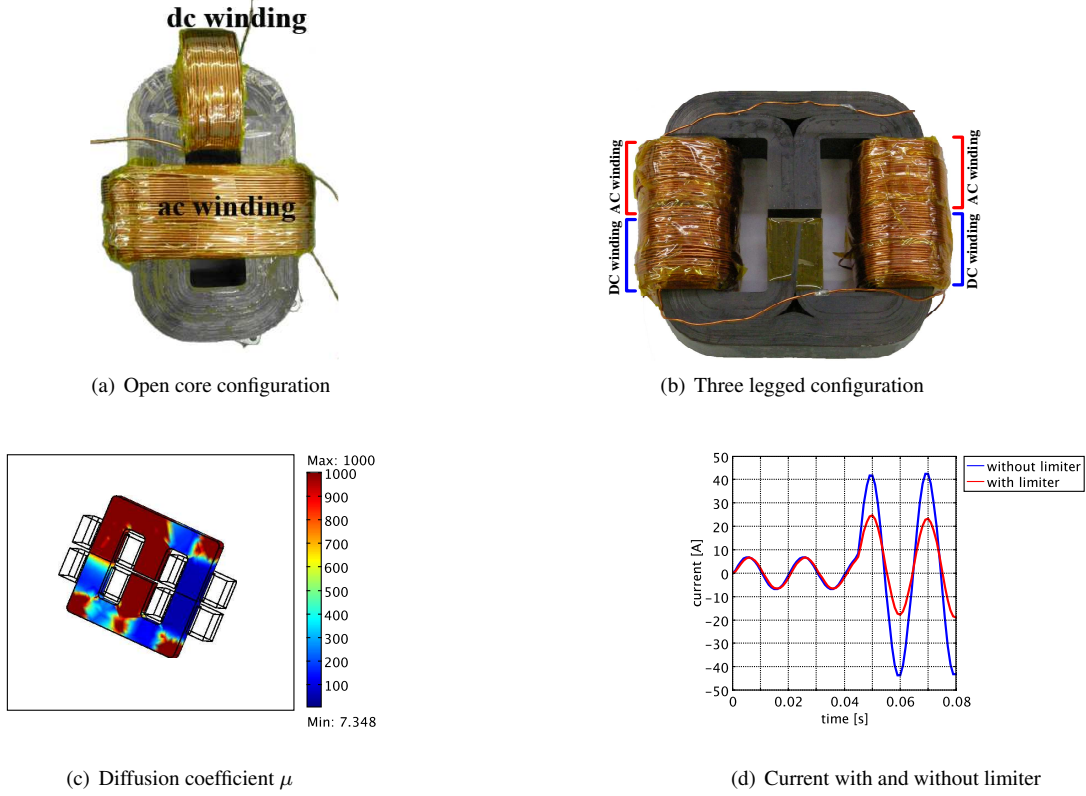


Figure 1.3: Numerical simulation of fault current limiters.

1.3 Classification of Second Order Partial Differential Equations

In this section we classify second order linear partial differential equations (PDEs) with constant coefficients according to their elliptic, parabolic and hyperbolic nature and give examples of PDEs in each of these three classes.

Classification We consider an open two-dimensional domain $(x, y) \in \Omega \subset \mathbb{R}^2$ with boundary $\Gamma = \partial\Omega$ as the domain of the second order linear partial differential equation (PDE) for the unknown field $u = u(x, y)$ and the source function $f(x, y)$ that can be written as

$$\mathcal{L}(u) = f \text{ on } \Omega \tag{1.1}$$

where the operator \mathcal{L} has constant coefficients a_{ij}, b_i and c

$$\mathcal{L}(u) = a_{11} \frac{\partial^2 u(x, y)}{\partial x^2} + 2a_{12} \frac{\partial^2 u(x, y)}{\partial x \partial y} + a_{22} \frac{\partial^2 u(x, y)}{\partial y^2} + b_1 \frac{\partial u(x, y)}{\partial x} + b_2 \frac{\partial u(x, y)}{\partial y} + c u(x, y). \tag{1.2}$$

We classify these equation based on the sign of the determinant

$$D = \begin{vmatrix} a_{11} & a_{12} \\ a_{12} & a_{22} \end{vmatrix} = a_{11}a_{22} - a_{12}^2. \tag{1.3}$$

The differential operator \mathcal{L} is called

- *elliptic* if $D > 0$
- *parabolic* if $D = 0$

- *hyperbolic* if $D < 0$

Prototypes in this classification are the elliptic Laplace equation $u_{xx} + u_{yy} = 0$, parabolic heat equation $u_{xx} - u_y = 0$ and the hyperbolic wave equation $u_{xx} - u_{yy} = 0$. In the case of xy -varying coefficients a_{11} , a_{22} and a_{12} , the sign of D and therefore the type of the PDE may change with the location in Ω .

As FEM solvers for discretized hyperbolic PDEs are far less developed, we will only consider elliptic and parabolic equations in this course. Elliptic equations are characterized by the fact that changes in the data imposed on the boundary Γ are felt instantaneously in the interior of Ω . Parabolic equations model the evolution of a system from initial to an stationary (time-independent) equilibrium state.

Examples of Elliptic Partial Differential Equations We will consider the Poisson equation

$$-\Delta u := -\frac{\partial^2 u(x, y)}{\partial x^2} - \frac{\partial^2 u(x, y)}{\partial y^2} = f \quad (1.4)$$

as it plays a central role in engineering applications in which the field u solved for plays the role of a (electric, magnetic or gravitational) potential, temperature or displacement. The reason for the minus sign in front of the Laplacian will be discussed together with the finite element discretization. We will also consider two variants of (1.4). In the first variant we introduce a small positive parameter $0 < \epsilon \ll 1$ to arrive at the anisotropic variant

$$-\epsilon \frac{\partial^2 u(x, y)}{\partial x^2} - \frac{\partial^2 u(x, y)}{\partial y^2} = f \quad (1.5)$$

that can be thought of as a simplified model to study the effect of local mesh refinement required to capture e.g. boundary layers or small geometrical details (such as for instance the air-gap in an electrical machine). In the second variant we again incorporate more physical realism in (1.4) by allowing the parameter c in

$$-\frac{\partial}{\partial x} \left(c \frac{\partial u(x, y)}{\partial x} \right) - \frac{\partial}{\partial y} \left(c \frac{\partial u(x, y)}{\partial y} \right) = f, \quad (1.6)$$

to have a jump-discontinuity across the boundary of two subdomains (such as for instance the jump in electrical conductivity across the interface between copper and air).

The Helmholtz and the convection-diffusion equation are other examples of elliptic partial differential equations. The former can be written as

$$-\Delta u - k^2 u = -\frac{\partial^2 u(x, y)}{\partial x^2} - \frac{\partial^2 u(x, y)}{\partial y^2} - k^2 u = f, \quad (1.7)$$

and models the propagation of an acoustical or electromagnetic wave with wave number k . The latter is a simplified model for the study of a flow with (dimensionless) velocity $\mathbf{v} = (1, 0)$ around a body and can be written as

$$-\epsilon \Delta u + \mathbf{v} \cdot \nabla u = -\epsilon \frac{\partial^2 u(x, y)}{\partial x^2} - \epsilon \frac{\partial^2 u(x, y)}{\partial y^2} + \frac{\partial u(x, y)}{\partial x} = f, \quad (1.8)$$

where ϵ is the inverse of the Peclet number (which plays the same role as the Reynolds number in the Navier-Stokes equations). The verification that the equations introduced above are indeed elliptic is left as an exercise.

The classification given above can be extended to systems of coupled partial differential equations. The vector-valued double curl equation for example relates the vector potential $\mathbf{U}(x, y, z) = (U_1(x, y, z), U_2(x, y, z), U_3(x, y, z))$ with the excitation vector field $\mathbf{F}(x, y, z)$ and can be written as

$$\nabla \times (\nu \nabla \times \mathbf{U}) = \mathbf{F}(x, y, z), \quad (1.9)$$

where as in (1.6) ν represents a material parameter. This model can be derived from the Maxwell equations and plays a central role in the finite element modeling of electrical machines, wind turbines and power transformers. In this setting \mathbf{F} and \mathbf{U} play the role of the applied current density and the magnetic vector potential, respectively.

In order to guarantee uniqueness of the solution of the above elliptic partial differential equations, appropriate (Dirichlet, Neumann or other) boundary conditions on $\Gamma = \partial\Omega$ need to be supplied.

Example of a Parabolic Partial Differential Equation In order to give examples of parabolic partial differential equations, we change the notation y into t and consider Ω to be a rectangle $(x, t) \in \Omega = [0, L] \times [0, T]$. The parabolic differential equation with source term $f(x, t)$

$$\frac{\partial u(x, t)}{\partial t} = \frac{\partial^2 u(x, t)}{\partial x^2} + f(x, t) \quad (1.10)$$

models the diffusion of the quantity $u(x, t)$ in time that reaches a time-independent equilibrium state when $\frac{\partial u(x, t)}{\partial t}$ is zero. All of the elliptic models introduced above can be extended to a parabolic model by adding the allowing u to become time-dependent, that is $u = u(x, y, t)$, and adding the term $\frac{\partial u(x, t)}{\partial t}$. These models will be considered for instance when discussing the role of initial vectors of iterative solution methods.

In order to guarantee uniqueness of the solution of parabolic partial differential equations, both boundary and initial conditions need to be supplied.

1.4 Model Problems

In this section we define a sequence of model problems for future reference.

Elliptic Problem Problems

- given the domain $\Omega = (a, b) \subset \mathbb{R}$ with boundary, given a positive diffusion coefficient $c(x) > 0, \forall x \in (a, b)$, and given the boundary data $g(x)$ or $h(x)$, solve for $u(x)$ the following ordinary differential equation

$$-\frac{d^2 u(x)}{dx^2} = f(x) \text{ on } \Omega \quad (1.11)$$

or

$$-\frac{d}{dx} \left(c(x) \frac{du(x)}{dx} \right) = f(x) \text{ on } \Omega \quad (1.12)$$

supplied with either Dirichlet boundary conditions

$$u(x) = g(x) \text{ on } x = a \text{ and/or } x = b \quad (1.13)$$

or Neumann boundary conditions

$$\frac{du(x)}{dx} = h(x) \text{ on } x = a \text{ and/or } x = b. \quad (1.14)$$

In case that $g(x) = 0$ in (1.13) ($h(x) = 0$ in (1.14)) the Dirichlet (Neumann) boundary conditions is called homogeneous.

- given an open and bounded domain $\Omega \subset \mathbb{R}^2$ with boundary $\Gamma = \partial\Omega$ that can be subdivided as $\Gamma = \Gamma_D \cup \Gamma_N$ and outward normal \mathbf{n} , given a positive diffusion coefficient $c(x, y) > 0, \forall (x, y) \in \Omega$, and given the boundary data $g(x, y)$ or $h(x, y)$, solve for $u(x, y)$ the following partial differential equation

$$-\Delta u := -\frac{\partial^2 u(x, y)}{\partial x^2} - \frac{\partial^2 u(x, y)}{\partial y^2} = f(x, y) \text{ on } \Omega, \quad (1.15)$$

or

$$-\frac{\partial}{\partial x} \left(c(x, y) \frac{\partial u(x, y)}{\partial x} \right) - \frac{\partial}{\partial y} \left(c(x, y) \frac{\partial u(x, y)}{\partial y} \right) = f(x, y) \text{ on } \Omega, \quad (1.16)$$

supplied with either Dirichlet boundary conditions

$$u(x, y) = g(x, y) \text{ on } \Gamma_D \quad (1.17)$$

or Neumann boundary conditions

$$\frac{\partial u(x, y)}{\partial n} = \nabla u(x, y) \cdot \mathbf{n} = h(x, y) \text{ on } \Gamma_N. \quad (1.18)$$

- double curl equation on a 3D domain

Chapter 2

Mathematical Preliminaries

The goals and motivations of this chapter are to

- generalize the concept of a primitive of a scalar function in a single real variable to vector-valued functions resulting in the concept of a (scalar or vector) potential;
- generalize the integration by parts formula for integrals of scalar functions to integrals of vector-valued functions allowing to cast the strong form of a partial differential equation problem into its weak (or variational) form;
- give the fundamental lemma of variational calculus as allowing to demonstrate the equivalence of the strong and weak form of a partial differential equation problem.

We refer to Stuart for details.

2.1 The Geometry of \mathbb{R}^3

We denote a point in the three-dimensional Euclidean space \mathbb{R}^3 by $\mathbf{x} = (x, y, z)$. We denote a vector \mathbf{u} in \mathbb{R}^3 either by its components (u_1, u_2, u_3) or by the (vectorial) sum of the components times the respective unit vectors in x , y and z -direction, i.e. $\mathbf{u} = u_1 \mathbf{i} + u_2 \mathbf{j} + u_3 \mathbf{k}$.

Inner product and norm We denote the *inner product* (or scalar product) of two vectors $\mathbf{u} = (u_1, u_2, u_3)$ and $\mathbf{v} = (v_1, v_2, v_3)$ in \mathbb{R}^3 by $\mathbf{u} \cdot \mathbf{v}$. The result of this product is a number (or scalar) defined as

$$\mathbf{u} \cdot \mathbf{v} = u_1 v_1 + u_2 v_2 + u_3 v_3. \quad (2.1)$$

The *norm* of the vector \mathbf{u} denoted as $\|\mathbf{u}\|$ is defined as

$$\|\mathbf{u}\| = \sqrt{\mathbf{u} \cdot \mathbf{u}} = \sqrt{u_1 u_1 + u_2 u_2 + u_3 u_3}. \quad (2.2)$$

Outer product We denote the *outer product* (or vector product) of two vectors $\mathbf{u} = (u_1, u_2, u_3)$ and $\mathbf{v} = (v_1, v_2, v_3)$ in \mathbb{R}^3 by $\mathbf{u} \times \mathbf{v}$. The result of this product is a vector defined as

$$\mathbf{u} \times \mathbf{v} = \begin{vmatrix} \mathbf{i} & \mathbf{j} & \mathbf{k} \\ u_1 & u_2 & u_3 \\ v_1 & v_2 & v_3 \end{vmatrix} = [u_2 v_3 - u_3 v_2] \mathbf{i} - [u_1 v_3 - u_3 v_1] \mathbf{j} + [u_1 v_2 - u_2 v_1] \mathbf{k}. \quad (2.3)$$

The *triple product* of three vectors \mathbf{u} , \mathbf{v} and \mathbf{w} is defined as $(\mathbf{u} \times \mathbf{v}) \cdot \mathbf{w}$ and satisfies

$$(\mathbf{u} \times \mathbf{v}) \cdot \mathbf{w} = \mathbf{u} \cdot (\mathbf{v} \times \mathbf{w}) \quad (2.4)$$

2.2 Calculus of Functions of a Real Variable

Assume $f(x)$ to be a scalar function in a single real variable x . A point x_0 in the domain of f such that $\frac{df}{dx}(x = x_0) = f'(x_0) = 0$ is called a critical point of $f(x)$. The function $f(x)$ attains its (local) minima and maxima in its first order critical points (though not all first order critical points are minima or maxima of $f(x)$). The Fundamental theorem of Calculus states that, given a function $f(x)$ in a single real variables with primitive $F(x)$, the integral $\int_a^b f(x) dx$ can be computed as

$$\int_a^b f(x) dx = F(b) - F(a). \quad (2.5)$$

The following integration by parts formula holds

$$\int_a^b f(x) g'(x) dx = [f(x)g(x)]_a^b - \int_a^b f'(x) g(x) dx. \quad (2.6)$$

2.3 Calculus of Functions of Several Variables

Assume $u(\mathbf{x}) = u(x, y, z)$ to be a function on \mathbb{R}^3 , i.e., $u(\mathbf{x}) : \mathbb{R}^3 \mapsto \mathbb{R}$. Assume furthermore \mathbf{x}_0 to be point in the domain of $u(\mathbf{x})$ and \mathbf{s} a unit vector, respectively.

Directional Derivative The derivative of $u(\mathbf{x})$ in the direction \mathbf{s} in the point \mathbf{x}_0 is denoted as $D_{\mathbf{s}}u(\mathbf{x}_0)$ and defined as

$$D_{\mathbf{s}}u(\mathbf{x}_0) = \lim_{\epsilon \rightarrow 0} \frac{u(\mathbf{x}_0 + \epsilon \mathbf{s}) - u(\mathbf{x}_0)}{\epsilon} = \frac{d}{d\epsilon} [u(\mathbf{x}_0 + \epsilon \mathbf{s})] |_{\epsilon=0}. \quad (2.7)$$

This derivative gives the rate of change $u(\mathbf{x}) = u(x, y, z)$ in the direction of \mathbf{s} at the point \mathbf{x}_0 .

Gradient The *gradient* of u denoted as $\text{grad } u = \nabla u$ is vector function that is defined as

$$\nabla u = \left(\frac{\partial u}{\partial x}, \frac{\partial u}{\partial y}, \frac{\partial u}{\partial z} \right) = \frac{\partial u}{\partial x} \mathbf{i} + \frac{\partial u}{\partial y} \mathbf{j} + \frac{\partial u}{\partial z} \mathbf{k} = u_x \mathbf{i} + u_y \mathbf{j} + u_z \mathbf{k}. \quad (2.8)$$

The gradient of u is allows to compute the directional derivative of u in the direction of \mathbf{s} . We indeed have that $D_{\mathbf{s}}u(\mathbf{x}_0) = \nabla u(\mathbf{x}_0) \cdot \mathbf{s}$. This identity will be useful in formulating necessary conditions for first order critical points of $u(\mathbf{x})$. In a physical context and in case that u is e.g. the temperature, ∇u is proportional to the heat flux.

First Order Critical Points The point \mathbf{x}_0 is a first order critical point of $u(\mathbf{x}_0)$ iff $\nabla u(\mathbf{x}_0) = \mathbf{0}$ in \mathbb{R}^3 . The latter condition can be stated equivalently as

$$\frac{d}{d\epsilon} [u(\mathbf{x}_0 + \epsilon \mathbf{s})] |_{\epsilon=0} = 0 \quad (\text{in } \mathbb{R}) \quad \forall \mathbf{s} \in \mathbb{R}^3 \text{ with } \|\mathbf{s}\| = 1. \quad (2.9)$$

This condition will be allow to define first order critical point of functionals on infinite dimensional vector spaces in the next chapter.

2.4 Calculus of Vector Functions

Assume $\mathbf{F}(\mathbf{x}) = (F_1(\mathbf{x}), F_2(\mathbf{x}), F_3(\mathbf{x}))$ to be a vector function on \mathbb{R}^3 , i.e., $\mathbf{F}(\mathbf{x}) : \mathbb{R}^3 \mapsto \mathbb{R}^3$.

Divergence and curl The *divergence* of \mathbf{F} denoted as $\text{div } \mathbf{F} = \nabla \cdot \mathbf{F}$ is a scalar function that is defined as

$$\nabla \cdot \mathbf{F} = \frac{\partial F_1}{\partial x} + \frac{\partial F_2}{\partial y} + \frac{\partial F_3}{\partial z}. \quad (2.10)$$

The *curl* (or rotation) of \mathbf{F} denoted as $\text{curl } \mathbf{F} = \nabla \times \mathbf{F}$ is a vector function that is defined as

$$\nabla \times \mathbf{F} = \begin{pmatrix} \frac{\partial F_3}{\partial y} - \frac{\partial F_2}{\partial z} \\ -\frac{\partial F_3}{\partial x} + \frac{\partial F_1}{\partial z} \\ \frac{\partial F_2}{\partial x} - \frac{\partial F_1}{\partial y} \end{pmatrix} = \left(\frac{\partial F_3}{\partial y} - \frac{\partial F_2}{\partial z} \right) \mathbf{i} - \left(\frac{\partial F_3}{\partial x} - \frac{\partial F_1}{\partial z} \right) \mathbf{j} + \left(\frac{\partial F_2}{\partial x} - \frac{\partial F_1}{\partial y} \right) \mathbf{k}. \quad (2.11)$$

The divergence of the vector field F evaluated at a particular point \mathbf{x} is the extent to which the vector field behaves like a source or a sink at a given point. If the divergence is nonzero at some point then there must be a source or sink at that position. The curl of a vector field \mathbf{F} describes an infinitesimal rotation of \mathbf{F} .

Example 2.4.1 Insert examples as in previous version of the ATHENS notes here.

Example 2.4.2 Assume $c(\mathbf{x})$ and $u(\mathbf{x})$ to be two scalar functions. Then $c \nabla u$ is a vector function whose divergence is equal to

$$\nabla \cdot (c \nabla u) = \frac{\partial}{\partial x} \left(c \frac{\partial u}{\partial x} \right) + \frac{\partial}{\partial y} \left(c \frac{\partial u}{\partial y} \right) + \frac{\partial}{\partial z} \left(c \frac{\partial u}{\partial z} \right). \quad (2.12)$$

If in particular $c = 1$ (i.e. $c(\mathbf{x}) = 1$ for all \mathbf{x}), then

$$\nabla \cdot \nabla u = \Delta u = \frac{\partial^2 u}{\partial x^2} + \frac{\partial^2 u}{\partial y^2} + \frac{\partial^2 u}{\partial z^2}, \quad (2.13)$$

where Δu denotes the Laplacian of u . This differential operator is generalized to vector-valued functions $\mathbf{F}(\mathbf{x})$ by the double-curl operator as $\nabla \times (c \nabla \times \mathbf{F})$.

Proposition 2.4.1 From the above definitions immediately follows that for any scalar function u and for any vector function \mathbf{F} that

$$\nabla \times (\nabla u) = \mathbf{0} \text{ (in } \mathbb{R}^3) \quad (2.14)$$

$$\nabla \cdot (\nabla \times \mathbf{F}) = 0 \text{ (in } \mathbb{R}). \quad (2.15)$$

We will see below that scalar functions u that satisfy $\nabla \cdot u = 0$ and vector functions \mathbf{F} that satisfy $\nabla \times \mathbf{F} = \mathbf{0}$ play a special role as they generalize the notion of a constant function $f(x)$ for which $f'(x) = 0$.

Proposition 2.4.2 Let c , u and v be scalar functions and let \mathbf{F} , \mathbf{G} and \mathbf{U} be vector functions. By applying the product rule for differentiation, the following properties can be derived

$$\nabla \cdot (v\mathbf{F}) = v \nabla \cdot \mathbf{F} + \nabla v \cdot \mathbf{F} \quad (2.16)$$

$$\nabla \cdot (\mathbf{F} \times \mathbf{G}) = (\nabla \times \mathbf{F}) \cdot \mathbf{G} + (\nabla \times \mathbf{G}) \cdot \mathbf{F}. \quad (2.17)$$

Setting in the former equality $\mathbf{F} = c(\nabla u)$, yields

$$\nabla \cdot [(c \nabla u)v] = [\nabla \cdot (c \nabla u)]v + c \nabla u \cdot \nabla v. \quad (2.18)$$

while putting in the latter equality $\mathbf{F} = c(\nabla \times \mathbf{U})$, yields

$$\nabla \cdot [c(\nabla \times \mathbf{U}) \times \mathbf{G}] = [\nabla \times (c \nabla \times \mathbf{U})] \cdot \mathbf{G} + (\nabla \times \mathbf{G}) \cdot (c \nabla \times \mathbf{U}). \quad (2.19)$$

Flux and first integration theorem Assume S to be an oriented surface in \mathbb{R}^3 with unit outward normal \mathbf{n} . We will denote by $-S$ the surface that coincides with S and has opposite orientation. The normal derivative on S of the function u denoted as u_n is defined as $u_n = \nabla u \cdot \mathbf{n}$. The *flux* of \mathbf{F} through S denoted as Φ is defined as the surface integral

$$\Phi = \int_S \mathbf{F} \cdot d\mathbf{S} = \int_S \mathbf{F} \cdot \mathbf{n} dS. \quad (2.20)$$

Assume the surface S to be closed and enclosing a volume V . We make this relation explicit by writing $S = S(V)$. The Gauss integration theorem states that

$$\int_{S(V)} \mathbf{F} \cdot d\mathbf{S} = \int_V \nabla \cdot \mathbf{F} dV. \quad (2.21)$$

Proposition 2.4.3 Assume as in Proposition 2.4.2 c , u and v to be scalar functions and \mathbf{F} , \mathbf{G} and \mathbf{U} to be vector functions. Applying Gauss' Theorem to the vector function $v\mathbf{F}$ and using (2.16) to expand the right-hand side yields

$$\int_{S(V)} \mathbf{F} v \cdot d\mathbf{S} = \int_V \nabla \cdot [\mathbf{F} v] dV = \int_V v \nabla \cdot \mathbf{F} dV + \int_V \nabla v \cdot \mathbf{F} dV. \quad (2.22)$$

Setting $\mathbf{F} = c(\nabla u)$ yields

$$\int_{S(V)} [c(\nabla u)] v \cdot d\mathbf{S} = \int_V v \nabla \cdot [c(\nabla u)] dV + \int_V \nabla v \cdot [c(\nabla u)] dV. \quad (2.23)$$

Using the notation $u_n = \nabla u \cdot \mathbf{n}$ for the normal derivative, one can write the integrand in the left-hand side as $[c(\nabla u)] v \cdot d\mathbf{S} = [c(\nabla u)] v \cdot \mathbf{n} dS = c u_n v dS$. After rearranging terms, we obtain the following integration by parts formula

$$\int_V [\nabla \cdot (c \nabla u)] v dV = \int_{S(V)} c u_n v dS - \int_V c \nabla u \cdot \nabla v dV. \quad (2.24)$$

Applying Gauss' Theorem to the vector function $\mathbf{F} \times \mathbf{G}$ and using (2.17) to expand the right-hand side yields

$$\int_{S(V)} \mathbf{F} \times \mathbf{G} \cdot d\mathbf{S} = \int_V \nabla \cdot (\mathbf{F} \times \mathbf{G}) dV = \int_V (\nabla \times \mathbf{F}) \cdot \mathbf{G} dV + \int_V (\nabla \times \mathbf{G}) \cdot \mathbf{F} dV. \quad (2.25)$$

We use the identity (2.4) to rewrite the integrand in the left-hand side as $\mathbf{F} \times \mathbf{G} \cdot d\mathbf{S} = (\mathbf{F} \times \mathbf{G}) \cdot \mathbf{n} dS = \mathbf{F} \cdot (\mathbf{G} \times \mathbf{n}) dS$. Setting $\mathbf{F} = c(\nabla \times \mathbf{U})$ and rearranging terms then yields

$$\int_V [\nabla \times (c \nabla \times \mathbf{U})] \cdot \mathbf{G} dV = \int_{S(V)} c(\nabla \times \mathbf{U}) \cdot (\mathbf{G} \times \mathbf{n}) dS - \int_V (c \nabla \times \mathbf{U}) \cdot (\nabla \times \mathbf{G}) dV. \quad (2.26)$$

In subsequent chapters, we will extensively use a two-dimensional variant of (2.24) in which an oriented surface Ω with outward normal \mathbf{n} in \mathbb{R}^2 (that later we will later call a computational domain) is bounded by a boundary $\Gamma = \partial\Omega$. In this case we the following integration by parts formula

$$\boxed{\int_{\Omega} [\nabla \cdot (c \nabla u)] v d\Omega = \int_{\Gamma(\Omega)} c u_n v d\Gamma - \int_{\Omega} c \nabla u \cdot \nabla v d\Omega,} \quad (2.27)$$

Divergence-Free Vector Fields and Existence of Vector Potentials A vector function \mathbf{F} is called *divergence-free* (or solenoidal) on $\Omega \subset \mathbb{R}^3$ if and only if $\nabla \cdot \mathbf{F}(\mathbf{x}) = 0$ (in \mathbb{R}) for all $\mathbf{x} \in \Omega$. Unless stated differently, we will call in these notes a vector function \mathbf{F} divergence-free if and only if it is divergence-free on $\Omega = \mathbb{R}^3$.

Gauss' theorem implies that the flux of a divergence-free vector field through a closed surface S is zero. Decomposing S as $S = S^+ + (-S^-)$, the flux of a divergence-free \mathbf{F} through S^+ and S^- can then be seen to be equal. Given that S was chosen arbitrarily, the flux of a divergence-free vector in *surface independent*. This surface-independent property allows in turn to demonstrate that for divergence-free vector fields a vector potential \mathbf{A} must exist such that

$$\boxed{\mathbf{F} = \nabla \times \mathbf{A}}, \quad (2.28)$$

or component-wise

$$F_1 = \left(\frac{\partial A_3}{\partial y} - \frac{\partial A_2}{\partial z} \right), F_2 = \left(-\frac{\partial A_3}{\partial x} + \frac{\partial A_1}{\partial z} \right) \text{ and } F_3 = \left(\frac{\partial A_2}{\partial x} - \frac{\partial A_1}{\partial y} \right). \quad (2.29)$$

Circulation and second integration theorem Assume Γ to be a *closed* oriented curve in \mathbb{R}^3 with unit tangential vector \mathbf{t} . We will denote by $-\Gamma$ the curve that coincides with Γ and has opposite orientation. The tangential derivative along Γ of the function u denoted as u_t is defined as $u_t = \nabla u \cdot \mathbf{t}$. The *circulation* of \mathbf{F} along Γ denoted as \mathcal{C} is defined as the line integral

$$\mathcal{C} = \int_{\Gamma} \mathbf{F} \cdot d\mathbf{\Gamma} = \int_{\Gamma} \mathbf{F} \cdot \mathbf{t} \, d\Gamma. \quad (2.30)$$

Assume that the curve Γ encloses a surface S and that this relation is written as $\Gamma(S)$. The Stokes' integration theorem states that

$$\int_{\Gamma(S)} \mathbf{F} \cdot d\mathbf{\Gamma} = \int_S (\nabla \times \mathbf{F}) \cdot d\mathbf{S}. \quad (2.31)$$

Curl-Free Vector Fields and Existence of Scalar Potentials A vector function \mathbf{F} is called *curl-free* (or irrotational) on $\Omega \subset \mathbb{R}^3$ if and only if $\nabla \times \mathbf{F}(\mathbf{x}) = \mathbf{0}$ (in \mathbb{R}^3) for all $\mathbf{x} \in \Omega$. Unless stated differently, we will call in these notes a vector function \mathbf{F} curl-free if and only if it is curl-free on $\Omega = \mathbb{R}^3$.

Stokes' theorem implies that the circulation of a curl-free vector field along a closed curve Γ is zero. Decomposing Γ as $\Gamma = \Gamma^+ + (-\Gamma^-)$, the line integral of a divergence-free \mathbf{F} along Γ^+ and Γ^- can then be seen to be equal. Given that Γ was chosen arbitrarily, the circulation of a curl-free vector is *path independent*. This path-independent property allows in turn to demonstrate that for curl-free vector fields a scalar potential u must exist such that

$$\boxed{\mathbf{F} = \nabla \cdot u}, \quad (2.32)$$

or component-wise

$$F_1 = \frac{\partial u}{\partial x}, F_2 = \frac{\partial u}{\partial y} \text{ and } F_3 = \frac{\partial u}{\partial z}. \quad (2.33)$$

Chapter 3

Minimization Problems and Differential Equations

A physical system evolves in such a way to minimize their internal energy. Newton's apple falls due to gravitation. The thermal or magnetic flux passes by preference through regions of high (thermal or magnetic) conductivity. Partial differential equations are derived from this principle. Instead of solving the differential problem directly it might therefore be more advantageous to consider an equivalent energy minimization problem. In this chapter we put the equivalence between partial differential equations and minimization problems in a more formal setting as it will serve as a tool to explain FEM to solve the former. In this chapter we aim at

1. give the fundamental lemma of variational calculus known as du Bois-Reymond's lemma;
2. derive the Euler-Lagrange equation whose solution describes a stationary point for a functional to be minimized;
3. use the above two ingredients to show how partial differential equations can be derived from a minimization problem;
4. show under which conditions a partial differential differential can be derived from a minimization problem.

3.1 Function Spaces, Differential Operators and Functionals

In this section we introduce ingredients allowing to describe minimization problems formally. We seek to describe that the orbit that the falling apple describes is an orbit that minimizes its energy.

3.1.1 Function Spaces

Definition 3.1.1 (Function space) Given Ω (a domain in \mathbb{R} , \mathbb{R}^2 or \mathbb{R}^3), a function space $V(\Omega)$ is a space of functions (in one, two or three variables) on Ω that satisfy some smoothness requirements and possibly boundary conditions.

The set $V(\Omega)$ is e.g. the set of all imaginable orbits of the Newton's apple. We impose sufficient smoothness conditions to allow to take derivatives of elements in $V(\Omega)$. If additionally boundary conditions are imposed, elements $V(\Omega)$ can be viewed as solutions of a partial differential equation supplied with boundary conditions. More formally, we can give the following examples:

Example 3.1.1 (One-Dimensional Domain) Given the open interval $\Omega = (a, b) \subset \mathbb{R}$, we will denote $\mathcal{C}^1(\Omega)$ the functions $u(x)$ with a continuous first derivative $u'(x)$. We denote the subset $\mathcal{C}_0^1(\Omega) = \{u \in \mathcal{C}^1(\Omega) \mid u(a) = 0 = u(b)\}$ of functions satisfying homogeneous Dirichlet boundary conditions.

Example 3.1.2 (Two-Dimensional Domain) In problems on two-dimensional domain, we will denote by $\Omega \subset \mathbb{R}^2$ an open and bounded domain with boundary $\Gamma = \partial\Omega$ that can be partitioned into distinct parts Γ_D and Γ_N , i.e., $\Gamma = \Gamma_D \cup \Gamma_N$. We associate with Γ_D and Γ_N that part of the boundary on which (possibly non-homogeneous) Dirichlet and Neumann (or Robin) boundary conditions are imposed, respectively. We will denote by $\mathcal{C}^1(\Omega)$ the functions $u(x, y)$ with a continuous first order partial derivatives u_x and u_y . We will denote the subset $\mathcal{C}_0^1(\Omega) = \{u \in \mathcal{C}^1(\Omega) \mid u|_{\Gamma_D} = 0\}$.

Treatment of boundary conditions The presence of the Neumann boundary conditions is not reflected in the above definition of $\mathcal{C}_0^1(\Omega)$. The condition $u|_{\Gamma_D} = 0$ is imposed even in case of non-homogenous Dirichlet boundary conditions. Only with the latter condition the above function spaces are vector space (closed for linear combinations) of infinite dimensions. These vector spaces can be endowed with a norm, thus becoming therefore Hilbert spaces.

3.1.2 Differential Operators

Assume that \mathcal{L} is a second order differential operator acting on elements of $V(\Omega)$ and let $u = 0$, i.e., $u(\mathbf{x}) = 0 \forall \mathbf{x} \in \Omega$, denote the zero element of $V(\Omega)$. It is obvious that $\mathcal{L}u = 0$. This trivial situation is excluded in the following definition.

Definition 3.1.2 (Positivity) The differential operator \mathcal{L} is positive on $V(\Omega)$ iff

$$\int_{\Omega} v(\mathcal{L}v) d\Omega > 0 \quad \forall v \in V(\Omega) \setminus \{0\}. \quad (3.1)$$

Observe that in the above definition the boundary conditions are taken into account by incorporating in the definition of $V(\Omega)$ and requiring that $v \in V(\Omega)$.

Example 3.1.3 The differential operator $\mathcal{L}v = -\frac{d^2v}{dx^2} = -v''(x)$ is positive on $\mathcal{C}_0^1((a, b))$. Indeed, using integration by parts and the homogeneous Dirichlet boundary conditions we have that

$$\int_{\Omega} v(\mathcal{L}v) d\Omega = - \int_a^b v(x) v''(x) dx = - \underbrace{[v(x) v'(x)]_a^b}_{=0} + \int_a^b v'(x) v'(x) dx > 0. \quad (3.2)$$

Example 3.1.4 Given on open and bounded subset $\Omega \subset \mathbb{R}^2$ and the coefficient $c(\mathbf{x}) > 0 \forall \mathbf{x} \in \Omega$, the differential operator $\mathcal{L}v = -\nabla \cdot (c\nabla v)$ is positive on $\mathcal{C}_0^1(\Omega)$.

Definition 3.1.3 (Self-adjointness) The differential operator \mathcal{L} is called self-adjoint (or symmetric) on $V(\Omega)$ iff

$$\int_{\Omega} v(\mathcal{L}u) d\Omega = \int_{\Omega} u(\mathcal{L}v) d\Omega \quad \forall u, v \in V(\Omega). \quad (3.3)$$

Example 3.1.5 The differential operator $\mathcal{L}v = -\frac{d^2v}{dx^2}$ is self-adjoint on $\mathcal{C}_0^1((a, b))$. This can be seen by integrating by parts twice and using the homogeneous boundary conditions.

Example 3.1.6 Given an open and bounded subset $\Omega \subset \mathbb{R}^2$ and the coefficient $c(\mathbf{x}) > 0 \forall \mathbf{x} \in \Omega$, the differential operator $\mathcal{L}v = -\nabla \cdot (c\nabla v)$ is self-adjoint on $\mathcal{C}_0^1(\Omega)$.

3.1.3 Functionals

Definition 3.1.4 (Functional) Given a function space $V(\Omega)$, a functional L is a mapping from $V(\Omega)$ onto \mathbb{R} , i.e., $L : V(\Omega) \mapsto \mathbb{R}$.

If $u \in V(\Omega)$ is an orbits of Newton's apple, then $L(u)$ can for instance represent the length of the orbit. If $u \in V(\Omega)$ is a temperature distribution in a region, then can for instance represent the average of the temperature. In the modeling of electrical machines the function u typically represents the (scalar or vector) magnetic potential and the force, torque, resistive heat and eddy current are examples of functionals in u . More formal examples are given below.

Example 3.1.7 (Distance in Flat Land) Let $V(\Omega)$ be the set of differentiable functions on the open interval (a, b) supplied with the additional conditions that $u(x = a) = u_a$ and $u(x = b) = u_b$. The graph of each element of $V(\Omega)$ is a path between the points (a, u_a) and (b, u_b) in \mathbb{R}^2 . The length $L(u)$ of each of these path can be computed by the line integral

$$L(u) = \int ds \tag{3.4}$$

where, given that $dy = u'(x) dx$,

$$ds^2 = dx^2 + dy^2 = [1 + u'(x)^2] dx^2 \Leftrightarrow ds = \sqrt{1 + u'(x)^2} dx, \tag{3.5}$$

and therefore

$$L(u) = \int_a^b \sqrt{1 + u'(x)^2} dx. \tag{3.6}$$

Example 3.1.8 (Mass-Spring System) Let $V(\Omega)$ be the set of differentiable functions on the open interval (a, b) describing the motion of a point (apple) with mass m vertically attached to a wall with a spring constant k (the independent variable $x \in (a, b)$ thus denotes time here). The instantaneous energy $E[u(x)]$ of the mass is the sum of the kinetic and potential energy $T[u(x)] = 1/2 m u'(x)^2$ and $V[u(x)] = 1/2 k u(x)^2$, i.e., $E[u(x)] = T[u(x)] - V[u(x)]$. The total energy is the functional $L(u)$ defined on $V(\Omega)$ as

$$L(u) = \int_a^b [T[u(x)] - V[u(x)]] dx = \int_a^b [1/2 m u'(x)^2 - 1/2 k u(x)^2] dx. \tag{3.7}$$

Example 3.1.9 (Abstract One-Dimensional Example) The previous example can be put in a more abstract setting by allowing $f(x, u, u')$ to be a function in three variables mapping from $(a, b) \times V(\Omega) \times V(\Omega)$ to \mathbb{R} with continuous partial derivatives. Given such a function f , we define the functional on $V(\Omega)$ as

$$L(u) = \int_a^b f(x, u, u') dx. \tag{3.8}$$

In the next example we establish the link we differential equations. In this example the function f represents the source term in the differential equation, the current in the modeling of fault-current limiter or the burner in the industrial furnace example. The function c and h will turn out later to be the diffusion coefficient and the non-homogeneous term in the Neumann boundary conditions, respectively.

Example 3.1.10 (Two-Dimensional Self-Adjoint Differential Equation) Given $\Omega \subset \mathbb{R}^2$ an open and bounded two-dimensional domain with boundary $\Gamma = \Gamma_D \cup \Gamma_N$, given c a positive function on Ω , given f a (not-necessarily smooth) function on Ω and given h a function on Γ_N , a functional on $C^1(\Omega)$ can be defined by

$$L(u) = \int_{\Omega} \left[1/2 \nabla u \cdot (c \nabla u) - fu \right] d\Omega + \int_{\Gamma_N} h(x, y) u d\Gamma. \tag{3.9}$$

It turns out in the last example L is linear and bounded (and therefore continuous).

3.1.4 Minimization of Functionals

In this subsection we seek to minimize to minimize functionals over the corresponding function space, i.e., to find arguments $\tilde{u} \in V(\Omega)$ that minimize L or

$$\text{find } \tilde{u} \in V(\Omega) \text{ such that } L(\tilde{u}) \leq L(u) \quad \forall u \in V(\Omega). \tag{3.10}$$

Solving this problem is generally hard, if not impossible at all. Local and global minimizers might be hard to distinguish and the global optimum might be non-unique. We therefore aim towards the less ambitious goal of seeking first order critical points of L . These points are defined for functionals in the same way as for functions in several variables. The point \tilde{u} is a first order critical point of L iff the directional derivative of L in \tilde{u} is zero in all possible directions.

For the definition of first order critical point to have sense, it is **important** that the space of possible directions used in the definition forms a vector space, i.e., that this space is closed for linear combinations. This requires the proper treatment of the non-homogeneous Dirichlet boundary conditions. Indeed, any linear combination of two functions u_1 and u_2 satisfying the non-homogeneous Dirichlet boundary conditions no longer satisfies them. This motivates the following definition of the subspace $V_0(\Omega)$ of $V(\Omega)$

$$V_0(\Omega) = \{v \in V(\Omega) | v|_{\Gamma_D} = 0\}. \quad (3.11)$$

In case that non-homogeneous Dirichlet boundary conditions are imposed the space $V_0(\Omega)$ forms a vector space, while $V(\Omega)$ does not.

The problem of finding (local) minimizers of L now reduces to

$$\text{find } \tilde{u} \in V(\Omega) \text{ such that } \frac{d}{d\epsilon} [L(\tilde{u} + \epsilon v)]|_{\epsilon=0} = 0 \quad \forall v \in V_0(\Omega). \quad (3.12)$$

Note that \tilde{u} and v not necessarily belong to the same space. We will refer to $V_0(\Omega)$ as the space of test functions. Only if L is convex, there is only one critical point that coincides in the global minimizer of L .

3.2 Calculus of Variations

en.wikipedia.org/wiki/Fundamental_lemma_of_calculus_of_variations

3.3 From Functionals to Differential Equations

In this section we illustrate how differential equations can be obtained by the minimizing of functionals. Given a functional L , we will carry out the following three-step procedure:

1. assume that \tilde{u} is a first-order critical point of L and express that \tilde{u} satisfies the condition (3.12);
2. integrate integrate-by-parts and exploit the homogeneous Dirichlet boundary conditions of $v \in V_0(\Omega)$;
3. apply du-Bois Reymond's Lemma to derive the differential equation for \tilde{u} .

In what follows we illustrate the above procedure using the examples of functionals given above.

3.3.1 Distance in Flat Land

In this subsection we illustrate the above procedure using the functional introduced in Example 3.1.7. Given $\Omega = (a, b)$, and given the function space $V(\Omega)$ and $V_0(\Omega)$ where

$$V(\Omega) = \{u(x) | u'(x) \text{ continuous on } \Omega, u(x=a) = u_a \text{ and } u(x=b) = u_b\} \quad (3.13)$$

and

$$V_0(\Omega) = \{v(x) | v'(x) \text{ continuous on } \Omega, v(x=a) = 0 \text{ and } v(x=b) = 0\}, \quad (3.14)$$

we seek to minimize $L(u) = \int_a^b \sqrt{1 + u'(x)^2} dx$ over $V(\Omega)$. We begin by recalling that

$$\frac{d}{d\epsilon} (\tilde{u} + \epsilon v) = (\tilde{u} + \epsilon v)' = \tilde{u}' + \epsilon v'. \quad (3.15)$$

Next we compute the left-hand side of (3.12)

$$\begin{aligned} \frac{d}{d\epsilon} [L(\tilde{u} + \epsilon v)] &= \frac{d}{d\epsilon} \left[\int_a^b \sqrt{1 + (\tilde{u}' + \epsilon v')^2} dx \right] \\ &= \int_a^b \frac{d}{d\epsilon} \sqrt{1 + (\tilde{u}' + \epsilon v')^2} dx \\ &= \int_a^b \frac{(\tilde{u}' + \epsilon v') v'}{\sqrt{1 + (\tilde{u}' + \epsilon v')^2}} dx. \end{aligned} \quad (3.16)$$

Therefore

$$\frac{d}{d\epsilon} [L(\tilde{u} + \epsilon v)]|_{\epsilon=0} = \int_a^b \frac{\tilde{u}' v'}{\sqrt{1 + (\tilde{u}')^2}} dx, \quad (3.17)$$

and using by integration by parts and the homogeneous Dirichlet boundary conditions on v we obtain

$$\frac{d}{d\epsilon} [L(\tilde{u} + \epsilon v)]|_{\epsilon=0} = \underbrace{\left[\frac{\tilde{u}' v}{\sqrt{1 + (\tilde{u}')^2}} \right]_{x=a}^{x=b}}_{=0} - \int_a^b \frac{d}{dx} \left[\frac{\tilde{u}'}{\sqrt{1 + (\tilde{u}')^2}} \right] v dx. \quad (3.18)$$

We expand the integrand in the right-hand side as

$$\begin{aligned} \frac{d}{dx} \left[\frac{\tilde{u}'}{\sqrt{1 + (\tilde{u}')^2}} \right] &= \frac{d}{d\tilde{u}'} \left[\frac{\tilde{u}'}{\sqrt{1 + (\tilde{u}')^2}} \right] \frac{d\tilde{u}'}{dx} \\ &= \left[\frac{1}{\sqrt{1 + (\tilde{u}')^2}} \right] \tilde{u}'' + \tilde{u}' \frac{d}{d\tilde{u}'} \left[(1 + (\tilde{u}')^2)^{-1/2} \right] \tilde{u}'' \\ &= \left[\frac{1 + (\tilde{u}')^2}{[1 + (\tilde{u}')^2]^{3/2}} \right] \tilde{u}'' - \left[\frac{(\tilde{u}')^2}{[1 + (\tilde{u}')^2]^{3/2}} \right] \tilde{u}'' \\ &= \frac{\tilde{u}''}{[1 + (\tilde{u}')^2]^{3/2}}, \end{aligned} \quad (3.19)$$

and therefore

$$\frac{d}{d\epsilon} [L(\tilde{u} + \epsilon v)]|_{\epsilon=0} = - \int_a^b \left[\frac{\tilde{u}''}{[1 + (\tilde{u}')^2]^{3/2}} \right] v dx. \quad (3.20)$$

The condition (3.12) that \tilde{u} is a critical point is therefore equivalent to

$$\int_a^b \left[\frac{\tilde{u}''}{[1 + (\tilde{u}')^2]^{3/2}} \right] v dx = 0 \quad \forall v \in V_0(\Omega). \quad (3.21)$$

By du-Bois Reymond's Lemma we can then assert that

$$\frac{\tilde{u}''}{[1 + (\tilde{u}')^2]^{3/2}} = 0 \text{ on } (a, b) \Leftrightarrow \tilde{u}'' = 0 \text{ on } (a, b), \quad (3.22)$$

which is the differential equation for \tilde{u} sought for.

This example is sufficiently simple to allow for an analytical solution for \tilde{u} . Indeed, the differential equation $\tilde{u}'' = 0$ on (a, b) supplied with the boundary conditions $u(x = a) = u_a$ and $u(x = b) = u_b$ yields the solution

$$\tilde{u}(x) = u_a + \frac{u_b - u_a}{b - a}(x - a), \quad (3.23)$$

which is a straight line interval in \mathbb{R}^2 between the points (a, u_a) and (b, u_b) . More important than the solution is to observe the fact that the differential equation for \tilde{u} can be obtained by minimizing a functional.

Smoothness Requirements on the Solution The minimization and differential equation problem impose different smoothness requirements on \tilde{u} . Indeed, while the former only requires the first order derivative to exist, the latter requires the existence of the second order derivative. We indeed used integration by parts in deriving the differential equation, elevating the derivative on \tilde{u} from one to two. This difference in smoothness requirements on \tilde{u} will turn out to be **important** in motivating the use of the FEM method in solving engineering problems of practical interest.

3.3.2 Abstract One-Dimensional Minimization Problem

In this subsection we apply the same procedure as before on the functional L described in Example 3.1.9. Given as before $\Omega = (a, b)$, and given the function space $V(\Omega)$ and $V_0(\Omega)$ where

$$V(\Omega) = \{u(x) | u'(x) \text{ continuous on } \Omega, u(x = a) = u_a\} \quad (3.24)$$

and

$$V_0(\Omega) = \{v(x) | v'(x) \text{ continuous on } \Omega, v(x = a) = 0\}, \quad (3.25)$$

we seek to minimize $L(u) = \int_a^b f(x, u, u') dx$ over $V(\Omega)$. Notice the absence of conditions at the end point of Ω in the definition of both $V(\Omega)$ and $V_0(\Omega)$. In our derivation we will also make use of the function space $W_0(\Omega) \subset V_0(\Omega)$ where

$$W_0(\Omega) = \{v(x) | v'(x) \text{ continuous on } \Omega, v(x = a) = 0 \text{ and } v(x = b) = 0\}. \quad (3.26)$$

We begin by computing the left-hand side of (3.12)

$$\begin{aligned} \frac{d}{d\epsilon} [L(\tilde{u} + \epsilon v)] &= \frac{d}{d\epsilon} \left[\int_a^b f(x, \tilde{u} + \epsilon v, \tilde{u}' + \epsilon v') dx \right] \\ &= \int_a^b \frac{d}{d\epsilon} f(x, \tilde{u} + \epsilon v, \tilde{u}' + \epsilon v') dx. \end{aligned} \quad (3.27)$$

The derivative in the integrand on the right-hand side can be computed via the chain rule, i.e.,

$$\begin{aligned} \frac{d}{d\epsilon} f(x, \tilde{u} + \epsilon v, \tilde{u}' + \epsilon v') &= \frac{\partial f}{\partial u}(x, \tilde{u} + \epsilon v, \tilde{u}' + \epsilon v') \frac{d(\tilde{u} + \epsilon v)}{d\epsilon} + \\ &\quad \frac{\partial f}{\partial u'}(x, \tilde{u} + \epsilon v, \tilde{u}' + \epsilon v') \frac{d(\tilde{u}' + \epsilon v')}{d\epsilon} \\ &= \frac{\partial f}{\partial u}(x, \tilde{u} + \epsilon v, \tilde{u}' + \epsilon v') v + \frac{\partial f}{\partial u'}(x, \tilde{u} + \epsilon v, \tilde{u}' + \epsilon v') v'. \end{aligned} \quad (3.28)$$

Substituting this result into the integral and splitting the integral into two parts, one obtains

$$\frac{d}{d\epsilon} [L(\tilde{u} + \epsilon v)] = \int_a^b \frac{\partial f}{\partial u}(x, \tilde{u} + \epsilon v, \tilde{u}' + \epsilon v') v dx + \int_a^b \frac{\partial f}{\partial u'}(x, \tilde{u} + \epsilon v, \tilde{u}' + \epsilon v') v' dx. \quad (3.29)$$

Therefore

$$\frac{d}{d\epsilon} [L(\tilde{u} + \epsilon v)]|_{\epsilon=0} = \int_a^b \frac{\partial f}{\partial u}(x, \tilde{u}, \tilde{u}') v dx + \int_a^b \frac{\partial f}{\partial u'}(x, \tilde{u}, \tilde{u}') v' dx. \quad (3.30)$$

and using by integration by parts and the homogeneous Dirichlet boundary conditions in $x = a$ on v we obtain

$$\begin{aligned} \frac{d}{d\epsilon} [L(\tilde{u} + \epsilon v)]|_{\epsilon=0} &= \int_a^b \frac{\partial f}{\partial u}(x, \tilde{u}, \tilde{u}') v dx + \underbrace{\left[\frac{\partial f}{\partial u'}(x, \tilde{u}, \tilde{u}') v \right]_{x=a}^{x=b}}_{=0 \text{ in } x=a \text{ only}} - \int_a^b \frac{d}{dx} \left[\frac{\partial f}{\partial u'}(x, \tilde{u}, \tilde{u}') \right] v dx \\ &= \int_a^b \frac{\partial f}{\partial u}(x, \tilde{u}, \tilde{u}') v dx + \frac{\partial f}{\partial u'}(x = b, \tilde{u}, \tilde{u}') v(x = b) - \int_a^b \frac{d}{dx} \left[\frac{\partial f}{\partial u'}(x, \tilde{u}, \tilde{u}') \right] v dx. \end{aligned} \quad (3.31)$$

The condition (3.12) is then seen to be equivalent to

$$\int_a^b \left[\frac{\partial f}{\partial u} - \frac{d}{dx} \left(\frac{\partial f}{\partial u'} \right) \right] v dx = \frac{\partial f}{\partial u'}(x = b, \tilde{u}, \tilde{u}') v(x = b) \quad \forall v \in V_0(\Omega). \quad (3.32)$$

At this point we can apply du-Bois Reymond's Lemma. The above condition should in particular hold for $v \in W_0(\Omega) \subset V_0(\Omega)$ for which $v(x = b) = 0$ and therefore

$$\int_a^b \left[\frac{\partial f}{\partial u} - \frac{d}{dx} \left(\frac{\partial f}{\partial u'} \right) \right] v dx = 0 \quad \forall v \in W_0(\Omega), \quad (3.33)$$

and therefore by du-Bois Reymond's Lemma

$$\frac{\partial f}{\partial u} - \frac{d}{dx} \left(\frac{\partial f}{\partial u'} \right) = 0 \text{ on } (a, b). \quad (3.34)$$

To treat the boundary condition as $x = b$ we return to larger space $V_0(\Omega)$ and to the relation (3.32) knowing now that the left-hand side is zero, i.e.,

$$\frac{\partial f}{\partial u'}(x = b, \tilde{u}, \tilde{u}') v(x = b) = 0 \quad \forall v \in V_0(\Omega), \quad (3.35)$$

and therefore we necessarily have that

$$\frac{\partial f}{\partial u'}(x = b, \tilde{u}, \tilde{u}') = 0. \quad (3.36)$$

Summarizing, we can state that the solution of the differential equation (3.34) supplied with the boundary conditions $u(x = a) = u_a$ and (3.36) minimizes $L(u) = \int_a^b f(x, u, u') dx$ over $V_0(\Omega)$. The minimization of a functional is seen to give raise to a partial differential equation with boundary conditions guaranteeing an unique solution.

The equation (3.34) is called the *Euler-Lagrange* equation. It plays an **important** role in various fields of physics such as geometrical optics, classical and quantum mechanics and cosmology as it allows to derive the governing equations starting from a functional describing the total energy of the system. This is illustrated in the example of Newton's apple in the next paragraph.

Newton's Apple In Example 3.1.8 the function $f(x, u, u')$ is seen to be

$$f(x, u, u') = 1/2 m u'(x)^2 - 1/2 k u(x)^2. \quad (3.37)$$

Therefore

$$\begin{aligned} \frac{\partial f}{\partial u'} &= m u'(x) \\ \frac{d}{dx} \left(\frac{\partial f}{\partial u'} \right) &= m u''(x) \\ \frac{\partial f}{\partial u} &= -k u(x). \end{aligned} \quad (3.38)$$

The Euler-Lagrange equation is therefore seen to simplify

$$m u''(x) = -k u(x), \quad (3.39)$$

which corresponds to the governing equation for a mass-spring system.

3.3.3 Two-Dimensional Self-Adjoint Problem

$$\begin{aligned} L(\tilde{u} + \epsilon v) &= \int_{\Omega} \left[1/2 \nabla(\tilde{u} + \epsilon v) \cdot [c \nabla(\tilde{u} + \epsilon v)] - f(\tilde{u} + \epsilon v) \right] d\Omega + \int_{\Gamma_N} h(x, y) (\tilde{u} + \epsilon v) d\Gamma \\ &= \int_{\Omega} \left[1/2 \nabla \tilde{u} \cdot (c \nabla \tilde{u}) - f \tilde{u} \right] d\Omega + \int_{\Gamma_N} h(x, y) \tilde{u} d\Gamma + \\ &\quad \epsilon \left[\int_{\Omega} \left[\nabla v \cdot (c \nabla \tilde{u}) - f v \right] d\Omega + \int_{\Gamma_N} h(x, y) v d\Gamma \right] + \epsilon^2 \int_{\Omega} 1/2 \nabla v \cdot (c \nabla v) d\Omega. \end{aligned} \quad (3.40)$$

Therefore

$$L(\tilde{u} + \epsilon v)|_{\epsilon=0} = \int_{\Omega} \left[\nabla v \cdot (c \nabla \tilde{u}) - f v \right] d\Omega + \int_{\Gamma_N} h(x, y) v d\Gamma \quad (3.41)$$

and using integration by parts and the homogeneous boundary conditions of v on Γ_D

$$\begin{aligned}
 L(\tilde{u} + \epsilon v)|_{\epsilon=0} &= \int_{\Omega} \nabla v \cdot (c \nabla \tilde{u}) v \, d\Omega - \int_{\Omega} f v \, d\Omega + \int_{\Gamma_N} h(x, y) v \, d\Gamma \\
 &= \int_{\Omega} \nabla \cdot (c \nabla \tilde{u}) v \, d\Omega - \int_{\Omega} f v \, d\Omega + \underbrace{\int_{\Gamma} c u_n v \, d\Gamma}_{v=0 \text{ on } \Gamma_D} + \int_{\Gamma_N} h(x, y) v \, d\Gamma \\
 &= \int_{\Omega} [\nabla \cdot (c \nabla \tilde{u}) - f] v \, d\Omega + \int_{\Gamma_N} [h(x, y) - c u_n] v \, d\Gamma
 \end{aligned} \tag{3.42}$$

3.4 From Differential Equation to Minimization Problem

Chapter 4

Quasi Stationary Magnetic Fields Models

4.1 Maxwell Equations

The starting point for deriving partial differential equation models for magnetic field computations are the Maxwell equations [1, 3]. These equations relate five vector fields: the magnetic field \mathbf{H} (units A/m), the magnetic flux density (or induction) \mathbf{B} (units T), the electric field \mathbf{E} (units V/m), the electric displacement \mathbf{D} (units) and the electric current density \mathbf{J} (units A/m^2). They can be written as

$$\nabla \times \mathbf{H} - \sigma \mathbf{v} \times \mathbf{B} = \mathbf{J} + \frac{\partial \mathbf{D}}{\partial t}, \quad (4.1)$$

$$\nabla \times \mathbf{E} = -\frac{\partial \mathbf{B}}{\partial t}, \quad (4.2)$$

$$\nabla \cdot \mathbf{B} = 0, \quad (4.3)$$

$$\nabla \cdot \mathbf{D} = \rho, \quad (4.4)$$

where ρ is the electric charge density and where \mathbf{v} is the velocity of the medium with electrical conductivity σ . Equations (4.12) and (4.13) are Ampère's law and Faraday's law respectively. Equations (4.14) and (4.4) are conservation laws. The Maxwell equations have to be completed with constitutive material equations

$$\mathbf{B} = \mu \mathbf{H}, \quad (4.5)$$

$$\mathbf{D} = \epsilon \mathbf{E}, \quad (4.6)$$

$$\mathbf{J} = \sigma \mathbf{E}, \quad (4.7)$$

where μ , ϵ and σ are the magnetic permeability and the electric permittivity and conductivity respectively. Equations (4.5) and (4.6) are the magnetic and dielectric relations, and equation (4.7) is Ohm's law. In the general case, the quantities μ , ϵ and σ are tensors. The law of charge conservation can be derived from the above equations. Indeed, given that $\nabla \cdot (\nabla \times \cdot) = 0$ for any vector field, taking the divergence of both sides of Ampère Law yields that

$$\frac{\partial \rho(\mathbf{x}, t)}{\partial t} + \nabla \cdot \mathbf{J}(\mathbf{x}, t) = 0, \quad (4.8)$$

which implies that in the absence of free charged particles implies that

$$\nabla \cdot \mathbf{J}(\mathbf{x}) = 0. \quad (4.9)$$

Maxwell's equations can be derived from a minimizing the electromagnetic energy

$$W_{tot}(t) = W_e(t) + W_m(t) \quad (4.10)$$

$$= \frac{1}{2} \int_{\Omega} \mathbf{D} \cdot \mathbf{E} d\Omega + \frac{1}{2} \int_{\Omega} \mathbf{B} \cdot \mathbf{H} d\Omega. \quad (4.11)$$

In the following sections the full set of Maxwell equations are reduced to simpler models by making assumptions on the time-behavior of the field and the dimensions of the problem.

4.2 Quasi-Stationary Approximation to Maxwell Equations

In a quasi-stationary approximation the displacement term can be neglected, and the Maxwell equations become

$$\nabla \times \mathbf{H} - \sigma \mathbf{v} \times \mathbf{B} = \mathbf{J}, \quad (4.12)$$

$$\nabla \times \mathbf{E} = -\frac{\partial \mathbf{B}}{\partial t}, \quad (4.13)$$

$$\nabla \cdot \mathbf{B} = 0, \quad (4.14)$$

4.3 Quasi-Stationary Approximation in Integral Form

Assume S as to be a (sufficiently smooth) oriented surface in \mathbb{R}^3 with unit outward normal vector \mathbf{n} . Assume furthermore S to be bounded by an oriented (sufficiently) smooth curve Γ with unit tangential vector \mathbf{t} . The surface integrals of \mathbf{B} and \mathbf{J} through S define the magnetic flux Φ and electric current I , respectively, i.e.,

$$\Phi = \int_S \mathbf{B} \cdot d\mathbf{s} = \int_S \mathbf{B} \cdot \mathbf{n} \, ds, \quad (4.15)$$

and

$$I = \int_S \mathbf{J} \cdot d\mathbf{s} = \int_S \mathbf{J} \cdot \mathbf{n} \, ds. \quad (4.16)$$

The surface integrals of $\nabla \times \mathbf{H}$ and $\nabla \times \mathbf{E}$ through S define the magnetic motive force (MMF) and electro motive force (EMF), respectively, i.e.,

$$\text{MMF} = \int_S (\nabla \times \mathbf{H}) \cdot d\mathbf{s} = \int_\Gamma \mathbf{H} \cdot d\mathbf{t} = \int_\Gamma \mathbf{H} \cdot \mathbf{t} \, d\gamma, \quad (4.17)$$

and

$$\text{EMF} = \int_S (\nabla \times \mathbf{E}) \cdot d\mathbf{s} = \int_\Gamma \mathbf{E} \cdot d\mathbf{t} = \int_\Gamma \mathbf{E} \cdot \mathbf{t} \, d\gamma. \quad (4.18)$$

In the absence of motion, the quasi static approximation to Maxwell equations can then be expressed as

$$\text{MMF} = I \quad (4.19)$$

$$\text{EMF} = -\frac{d\Psi}{dt}. \quad (4.20)$$

4.4 Stationary Approximation

In a stationary regime, the magnetic field quantities are decoupled from the electric ones and governed by

$$\nabla \times \mathbf{H}(\mathbf{x}) - \sigma \mathbf{v} \times \mathbf{B}(\mathbf{x}) = \mathbf{J}(\mathbf{x}), \quad (4.21)$$

$$\nabla \cdot \mathbf{B}(\mathbf{x}) = 0, \quad (4.22)$$

$$\mathbf{B}(\mathbf{x}) = \mu \mathbf{H}(\mathbf{x}). \quad (4.23)$$

(need to add physical dimensions).

Constitutive Equations The constitute equation (4.23) codes magnetic material properties into the magnetic field equations (4.28)-(4.22) and needs to be made more specific for the different materials considered. In the following we do so for the following frequently used materials:

- vacuum

$$\mathbf{B} = \mu_0 \mathbf{H}, \quad (4.24)$$

where the magnetic permeability of vacuum equals $\mu_0 = 4\pi \times 10^{-7} \frac{N}{A^2}$;

- linear ferromagnetic materials (e.g. linear steel)

$$\mathbf{B} = \mu \mathbf{H} = \mu_0 \mu_r \mathbf{H}, \quad (4.25)$$

where μ_r is the (constant) relative magnetic permeability;

- non-linear ferromagnetic materials (e.g. non-linear steel). For these materials the permeability (permeability tensor components) is a function of the magnitude (or strength) of the magnetic field denoted by B

$$\mathbf{B} = \mu(B) \mathbf{H} = \mu_0 \mu_r(B) \mathbf{H}, \quad (4.26)$$

where μ_r is the relative magnetic permeability. This relationship modeling magnetic saturation will be further discussed in subsequent chapters;

- permanent magnetic materials: different ways to model these materials exist. Using the remanent magnet flux density \mathbf{B}_r for instance, we have that

$$\mathbf{B} = \mu_0 \mu_r \mathbf{H} + \mathbf{B}_r. \quad (4.27)$$

Introducing of Potential Potential is a primitive for a vector field.

Scalar Potential Formulation By introducing either a scalar or magnetic vector potential, these equations transform into second order partial differential equations. In the absence of motion we have that $\mathbf{v} = 0$ and Equation (4.28) states that electrical charges moving uniformly in time give rise to a static magnetic field. If in addition $\mathbf{J} = 0$ and permanent magnet materials are present, then the curl-free condition for the magnetic field \mathbf{H} (4.28) is ensured by expressing \mathbf{H} in terms of the scalar magnetic potential V_m as

$$\mathbf{H} = \nabla V_m. \quad (4.28)$$

The substitution of (4.28) and (4.23) into (4.22) yields

$$\nabla \cdot (\mu \nabla V_m) = -\nabla \cdot \mathbf{B}_r, \quad (4.29)$$

where we brought the known vector \mathbf{B}_r to the right-hand side. In two-dimensional cartesian (xy) configurations with the direction of the of the magnetization in this plane, we can assume that $\mathbf{B}_r = (B_{rx}(x, y), B_{ry}(x, y), 0)$. This implies that the magnetic field reduces to $\mathbf{H} = (H_x(x, y), H_y(x, y), 0)$ where

$$H_x(x, y) = \frac{\partial V_m}{\partial x} \text{ and } H_y(x, y) = \frac{\partial V_m}{\partial y} \quad (4.30)$$

which in turn implies that the magnetic flux reduces to $\mathbf{B} = (B_x(x, y), B_y(x, y), 0)$ where

$$B_x(x, y) = \mu H_x(x, y) + B_{rx}(x, y) = \mu \frac{\partial V_m}{\partial x} + B_{rx}(x, y) \quad (4.31)$$

$$B_y(x, y) = \mu H_y(x, y) + B_{ry}(x, y) = \mu \frac{\partial V_m}{\partial y} + B_{ry}(x, y), \quad (4.32)$$

and the PDE for the scalar potential becomes

$$\frac{\partial}{\partial x} \left(\mu \frac{\partial V_m}{\partial x} \right) + \frac{\partial}{\partial y} \left(\mu \frac{\partial V_m}{\partial y} \right) = -\frac{\partial B_{rx}}{\partial x} - \frac{\partial B_{ry}}{\partial y}. \quad (4.33)$$

Vector Potential Formulation The divergence-free condition for the for the magnetic flux density \mathbf{B} (4.22) is ensured by expressing \mathbf{B} in terms of the magnetic vector potential \mathbf{A} as

$$\mathbf{B} = \nabla \times \mathbf{A} . \quad (4.34)$$

or

$$\mathbf{B} = (B_x(x, y, z), B_y(x, y, z), B_z(x, y, z)) \quad (4.35)$$

$$= \left(\frac{\partial A_z}{\partial y} - \frac{\partial A_y}{\partial z}, -\frac{\partial A_z}{\partial x} + \frac{\partial A_x}{\partial z}, \frac{\partial A_y}{\partial x} - \frac{\partial A_x}{\partial y} \right) . \quad (4.36)$$

The substitution of (4.34) and (4.23) into (4.28) in the presence of motion and the absence of permanent magnet materials yields

$$\nabla \times (\nu \nabla \times \mathbf{A}) - \sigma \mathbf{v} \times (\nabla \times \mathbf{A}) = \mathbf{J} , \quad (4.37)$$

where $\nu = 1/\mu$ is the magnetic reluctivity. In the absence of motion and presence of permanent magnetic materials one obtains

$$\nabla \times (\nu \nabla \times \mathbf{A}) = \mathbf{J} + \nu \nabla \times \mathbf{B}_r , \quad (4.38)$$

Equations (4.37) and (4.38) are coupled systems of three second order PDEs for the three components of \mathbf{A} . Once this system has been solved for \mathbf{A} , the technically relevant fields \mathbf{B} and \mathbf{H} can be calculated by relations (4.34) and (4.23).

To avoid the complexity of solving (4.37) or (4.38), two-dimensional approximations are often considered in engineering practice. We will consider perpendicular and in plane current formulations. We will consider the former in both cartesian and cylindrical coordinates. In many applications, these formulations already give valuable information of the device under consideration.

4.4.1 Perpendicular Current Formulation

In two-dimensional Cartesian formulations, the problem is posed on a domain Ω lying in the xy -plane and all field quantities are assumed to be z -independent. Here Ω models for example the cross-section perpendicular to the axis of an electrical machine. The current density \mathbf{J} is assumed to be perpendicular to Ω

$$\mathbf{J} = (0, 0, J_z(x, y)) , \quad (4.39)$$

and the remanent flux density is assumed to have components in Ω only

$$\mathbf{B}_r = (B_x(x, y), B_y(x, y), 0) . \quad (4.40)$$

Due to symmetry, the field quantity \mathbf{B} lies in the plane Ω

$$\mathbf{B} = (B_x(x, y), B_y(x, y), 0) . \quad (4.41)$$

Condition (4.34) can therefore be met assuming a potential \mathbf{A} of the form

$$\mathbf{A} = (0, 0, A_z(x, y)) . \quad (4.42)$$

and by (4.22) the components of \mathbf{B} can be expressed as

$$B_x = \frac{\partial A_z}{\partial y} \text{ and } B_y = -\frac{\partial A_z}{\partial x} . \quad (4.43)$$

Using appropriate constitutive equations, the components of the magnetic field can be expressed as

$$H_x(x, y) = \nu B_x(x, y) - \nu B_{rx}(x, y) = \nu \frac{\partial A_z}{\partial y} - \nu B_{rx}(x, y) \quad (4.44)$$

$$H_y(x, y) = \nu B_y(x, y) - \nu B_{ry}(x, y) = -\nu \frac{\partial A_z}{\partial x} - \nu B_{ry}(x, y) . \quad (4.45)$$

Moving Parts and No Permanent Magnet Materials By the above assumptions, the system (4.37) reduces to a single second order PDE for the z -component of the magnetic vector potential

$$-\frac{\partial}{\partial x} \left(\nu \frac{\partial A_z}{\partial x} \right) - \frac{\partial}{\partial y} \left(\nu \frac{\partial A_z}{\partial y} \right) + \sigma v_x \frac{\partial A_z}{\partial x} + \sigma v_y \frac{\partial A_z}{\partial y} = J_z . \quad (4.46)$$

No Moving Parts and With Permanent Magnet Materials By the above assumptions, the system (4.38) reduces to

$$-\frac{\partial}{\partial x} \left(\nu \frac{\partial A_z}{\partial x} \right) - \frac{\partial}{\partial y} \left(\nu \frac{\partial A_z}{\partial y} \right) = J_z + \nu \frac{\partial B_{ry}}{\partial x} - \nu \frac{\partial B_{rx}}{\partial y} . \quad (4.47)$$

Boundary conditions The above PDE for $A_z(x, y)$ need to be supplied with appropriate boundary conditions. We distinguish the following types

- magnetic insulation: $A_z(x, y) = 0$
- electric insulation:
- periodic boundary conditions:

Example 4.4.1 In Figure 4.4.1 we consider a permanent magnet magnetized in vertical direction and show the equipotential lines of the computed magnetic scalar and vector potential.

More examples Rotary electrical machines, linear actuators, transformers, shape optimization involving permanent magnets.

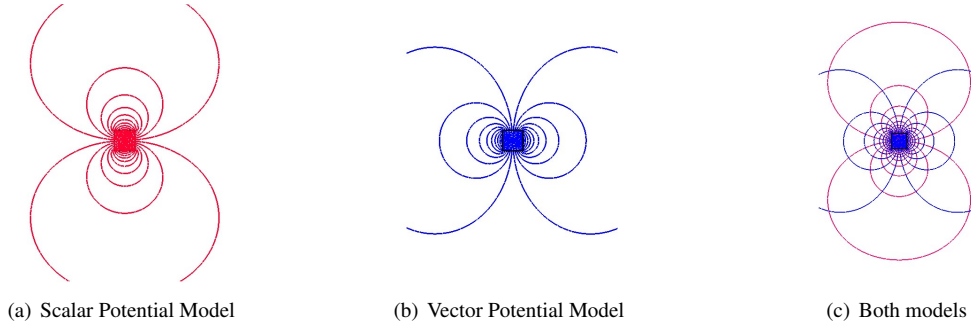


Figure 4.1: Perpendicular current model of a permanent magnet using both the scalar and vector magnetic potential.

4.4.2 Azimuthal Current Formulation

In an axi-symmetrical formulation in cylinder coordinates (r, θ, z) , the domain Ω lies in the rz -plane and all field quantities are assumed to be θ -independent. In analogy to the Cartesian formulation, the applied current density is assumed to be perpendicular to Ω

$$\mathbf{J} = (0, J_\theta(r, z), 0) . \quad (4.48)$$

As before the field quantity \mathbf{B} only has components in the modeling plane

$$\mathbf{B} = (B_r(r, z), 0, B_z(r, z)) . \quad (4.49)$$

Condition (4.34) can therefore be met assuming a potential \mathbf{A} of the form

$$\mathbf{A} = (0, A_\theta(r, z), 0) . \quad (4.50)$$

and by (4.22) in cylindrical coordinates

$$\nabla \times \mathbf{F} = \left(\frac{1}{r} \frac{\partial F_z}{\partial \theta} - \frac{\partial F_\theta}{\partial z}, \frac{\partial F_r}{\partial z} - \frac{\partial F_z}{\partial r}, \frac{1}{r} \left[\frac{\partial(rF_\theta)}{\partial r} - \frac{\partial F_r}{\partial \theta} \right] \right) \quad (4.51)$$

the components of \mathbf{B} in can be expressed as

$$B_r = -r \frac{\partial}{\partial z} \left(\frac{A_\theta(r, z)}{r} \right) = -\frac{\partial A_\theta(r, z)}{\partial z} \quad (4.52)$$

and

$$\begin{aligned} B_z &= r \frac{\partial}{\partial r} \left(\frac{A_\theta(r, z)}{r} \right) + 2 \frac{A_\theta(r, z)}{r} \\ &= r \frac{1}{r} \frac{\partial A_\theta(r, z)}{\partial r} - r A_\theta(r, z) \frac{1}{r^2} + 2 \frac{\partial A_\theta(r, z)}{r} \\ &= \frac{\partial A_\theta(r, z)}{\partial r} + \frac{\partial A_\theta(r, z)}{r} \\ &= \frac{1}{r} \left[\frac{\partial}{\partial r} (r A_\theta(r, z)) \right] \\ &= \frac{1}{r} \left[A_\theta(r, z) + r \frac{\partial}{\partial r} A_\theta(r, z) \right] \\ &= \frac{A_\theta(r, z)}{r} + \frac{\partial A_\theta(r, z)}{\partial r} \end{aligned} \quad (4.53)$$

The system (4.37) then reduces to the scalar equation

$$-\frac{\partial}{\partial r} \left(\nu \frac{\partial(r A_\theta)}{\partial r} \right) - \frac{\partial}{\partial z} \left(\nu \frac{\partial A_\theta}{\partial z} \right) + \sigma v_r \frac{\partial A_\theta}{\partial r} + \sigma v_z \frac{\partial A_\theta}{\partial z} = J_\theta. \quad (4.54)$$

Boundary condition Boundary condition on the axis of symmetry.

Examples Voice-coil actuator

The PDE in form (4.47) or (4.54) is the governing PDE for two-dimensional stationary magnetic field computations.

4.4.3 In Plane Current Formulation

Assume current flowing in plane

$$\mathbf{J} = (J_x(x, y), J_y(x, y), 0). \quad (4.55)$$

Then \mathbf{B} only has component perpendicular to the modeling plane

$$\mathbf{B} = (0, 0, B_z(x, y)). \quad (4.56)$$

Condition (4.34) can therefore be met assuming a potential \mathbf{A} of the form

$$\mathbf{A} = (A_x(x, y), A_y(x, y), 0), \quad (4.57)$$

and the B_z can be expressed as

$$B_z(x, y) = \frac{\partial A_y}{\partial x} - \frac{\partial A_x}{\partial y}. \quad (4.58)$$

The system (??) then reduces to the system of two coupled partial differential equations for $A_x(x, y)$ and $A_y(x, y)$

$$\frac{\partial}{\partial y} \nu \left(\frac{\partial A_y}{\partial x} - \frac{\partial A_x}{\partial y} \right) = J_x(x, y) \quad (4.59)$$

$$-\frac{\partial}{\partial x} \nu \left(\frac{\partial A_y}{\partial x} - \frac{\partial A_x}{\partial y} \right) = J_y(x, y) \quad (4.60)$$

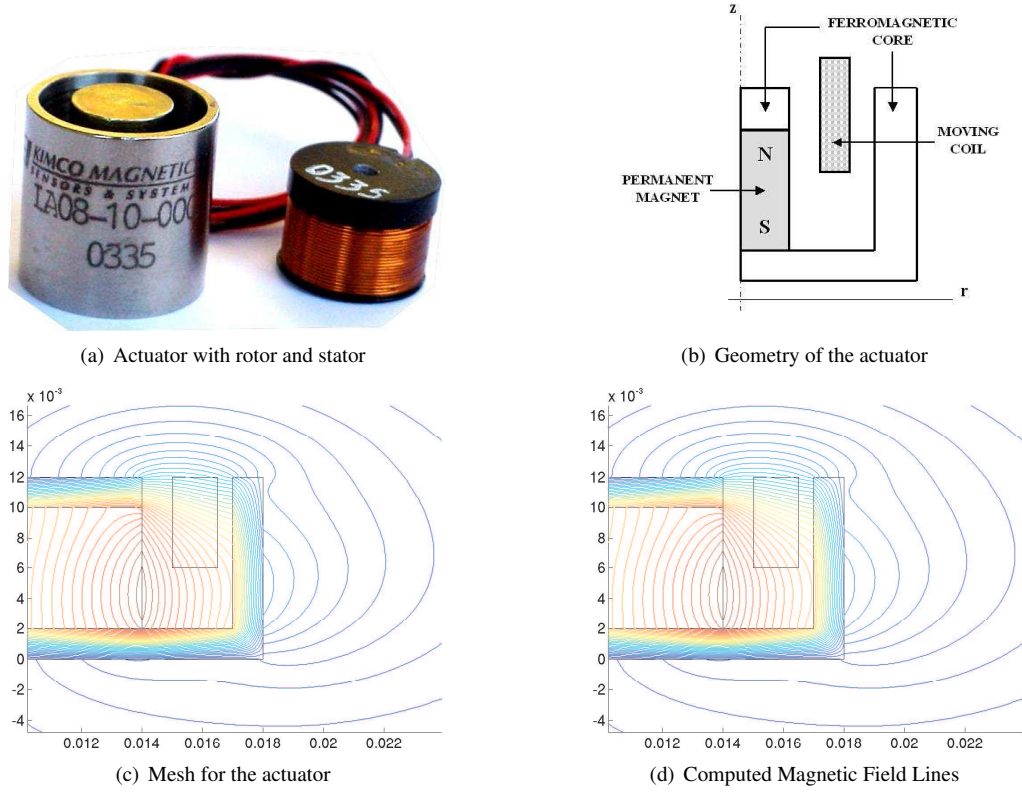


Figure 4.2: Axi-symmetrical vector-potential model of a voice-coil actuator.

Example Non-destructive testing of metallic structures using eddy currents. See example in Comsol Users Conference.

4.5 Transient Formulation

In order to derive the time-dependent magnetic field formulation, we eliminate the current density \mathbf{J} and the displacement current \mathbf{D} in the right-hand side of Ampère's law (4.12) using Ohm's law (4.7) and the dielectric relation (4.6) respectively. These manipulations yield

$$\nabla \times \mathbf{H} = \sigma \mathbf{E} + \epsilon \frac{\partial \mathbf{E}}{\partial t}. \quad (4.61)$$

We assume the electro-magnetic excitations, and thus also the induced electro-magnetic fields, to vary periodically in time with period T and with frequency $f = 1/T$. We introduce the dimensionless variable $t' = t/T = ft$. By rewriting the time derivative in the right-hand of (4.61) in this dimensionless variable, we obtain

$$\nabla \times \mathbf{H} = \sigma \mathbf{E} + \epsilon f \frac{\partial \mathbf{E}}{\partial t'}. \quad (4.62)$$

We assume the time-variations to be *quasi-stationary*. This assumption is justified by the fact that in technically relevant simulations of electro-magnetic energy transducers a sufficiently large upper bound on the frequency is

$$f \leq 10^4 \text{ Hz} . \quad (4.63)$$

For the electrically conducting media that we will consider, the electric conductivity σ and permeability ϵ lie in the ranges

$$\sigma \in [0, 10^9] \text{ C}^2 \text{ N}^{-1} \text{ m}^{-2} \text{ s}^{-1} \text{ and } \epsilon \in [\epsilon_0, 10 \epsilon_0], \quad (4.64)$$

where $\epsilon_0 = 8.85 \cdot 10^{-12} C^2 N^{-1} m^{-2}$ is the permittivity of vacuum. The above bounds on f , σ and ϵ allow us to neglect the contribution of the displacement current, i.e. the second term in the right-hand side of (4.62). Hence, we obtain

$$\nabla \times \mathbf{H} = \sigma \mathbf{E}. \quad (4.65)$$

In the presence of time-varying fields, the definition (4.34) for the vector potential \mathbf{A} remains valid. Introducing \mathbf{A} in the left-hand side of (4.65) yields

$$\nabla \times (\nu \nabla \times \mathbf{A}) = \sigma \mathbf{E}. \quad (4.66)$$

By Ohm's law (4.7), this equation can be written as

$$\nabla \times (\nu \nabla \times \mathbf{A}) = \mathbf{J}. \quad (4.67)$$

In the presence of time-varying fields, the integration of Faraday's law (4.13) yields

$$\mathbf{E} = -\nabla\phi - \frac{\partial \mathbf{A}}{\partial t}, \quad (4.68)$$

where the gradient of the electric potential $\nabla\phi$ is an integration constant. The contributions of the two terms in the right-hand side of (4.68) to the current distribution will be treated separately. Substituting (4.68) into the right-hand side of (4.7) yields

$$\mathbf{J} = \mathbf{J}_s + \mathbf{J}_e \quad \mathbf{J}_s = -\sigma \nabla\phi \quad \mathbf{J}_e = -\sigma \frac{\partial \mathbf{A}}{\partial t}, \quad (4.69)$$

where \mathbf{J}_s and \mathbf{J}_e are the source and induced (or eddy) current density respectively. Substituting (4.69) into the right-hand side of (4.66), we obtain the following partial differential equation for the vector potential

$$\sigma \frac{\partial \mathbf{A}}{\partial t} + \nabla \times (\nu \nabla \times \mathbf{A}) = \mathbf{J}_s. \quad (4.70)$$

4.6 Time-Harmonic Formulation

Solving the PDE (4.70) numerically entails a time-stepping procedure of some kind. In practice, a great deal of useful information can already be gained by assuming that the electromagnetic fields vary sinusoidally in time. Assuming a pulsation $\omega = 2\pi f$, we can write a generic electro-magnetic quantity $F(\mathbf{x}, t)$ oscillating harmonically in time as

$$F(\mathbf{x}, t) = \Re[\widehat{F}(\mathbf{x}) \exp(j\omega t)], \quad (4.71)$$

where the magnitude \widehat{F} is a complex-valued quantity consisting of a real and imaginary part $\Re[\widehat{F}]$ and $\Im[\widehat{F}]$ respectively. In a time-harmonic formulation, the PDEs (4.67) and (4.70) reduce to the following PDE for the amplitude $\widehat{\mathbf{A}}$ of the vector potential

$$\nabla \times (\nu \nabla \times \widehat{\mathbf{A}}) = \widehat{\mathbf{J}} \quad (4.72)$$

and

$$\nabla \times (\nu \nabla \times \widehat{\mathbf{A}}) + j\omega\sigma \widehat{\mathbf{A}} = \widehat{\mathbf{J}}_s \quad (4.73)$$

respectively. By a reasoning analogous to the derivation of equation (4.47), we reduce the system of coupled PDEs (4.72) and (4.73) to a scalar PDE. In the former case we obtain the Poisson equation

$$-\frac{\partial}{\partial x} \left(\nu \frac{\partial \widehat{A}_z}{\partial x} \right) - \frac{\partial}{\partial y} \left(\nu \frac{\partial \widehat{A}_z}{\partial y} \right) = \widehat{J}_z \quad (4.74)$$

while in the latter a Helmholtz equation with complex shift

$$-\frac{\partial}{\partial x} \left(\nu \frac{\partial \widehat{A}_z}{\partial x} \right) - \frac{\partial}{\partial y} \left(\nu \frac{\partial \widehat{A}_z}{\partial y} \right) + j\omega\sigma \widehat{A}_z = \widehat{J}_{s,z}, \quad (4.75)$$

where $\widehat{J}_{s,z}$ denotes the z -component of the source current density $\widehat{\mathbf{J}}_s$. Equations (4.74) and (4.75) are the governing PDEs for two-dimensional time-harmonic magnetic field formulations. In Section 4.8 we will argue which circumstances motivate the choice for either one of these equations.

In (4.71) we assumed a single frequency oscillatory behavior. In more advanced formulations a small set a discrete frequencies is taken into account. Such formulations are called *multi-harmonic* [?, ?].

4.7 Conductor Models

To do

- extends this part to the transient case
- include text on the impedance

Time-varying currents in a conductor magnetically induce eddy currents and voltages trying to counteract their source. The current will redistribute in such a way that the current density is larger towards the cross-section boundaries. This effect is known as the skin-effect and characterized by the skin-depth. The skin-depth δ is typical length scale measuring the size of the second order term relative to the term of order zero in the PDE (4.75) and is defined as

$$\delta = \sqrt{\frac{1}{\pi f \sigma \mu}}. \quad (4.76)$$

It is represented schematically in Figure ?? . Technically speaking, about 60% of the current flows in the shaded area in this figure. Different conductor models are distinguished based on the ratio between the skin-depth and the conductor radius, i.e. on the importance of the skin-effect in modeling the conductor. In this thesis we will consider *solid* and *stranded* conductors. For both conductor models and for time-varying field, one obtains by substituting (7.7) into (4.69) the relation

$$\widehat{J}_z = \frac{\sigma}{\ell_z} \widehat{\Delta V} - j \omega \sigma \widehat{A}_z \quad (4.77)$$

or, equivalently,

$$\widehat{\Delta V} = \ell_z \left(\frac{\widehat{J}_z}{\sigma} + j \omega \widehat{A}_z \right). \quad (4.78)$$

Subscripts *sol* and *str* will be used to indicate properties associated with the solid and stranded conductors respectively.

4.7.1 Solid Conductors

To add

1. the example in CMP
2. the proximity effect

A solid conductor is a massive bar of electrically conducting material with homogeneous cross-section Ω_{sol} . The radius of a solid conductor is large compared with the skin-depth δ . The variation of the current density over Ω_{sol} can therefore not be neglected. The magnitude of the voltage drop $\widehat{\Delta V}_{sol}$ in contrast is constant over Ω_{sol} .

Rotor bars in an induction machine are typically modeled as solid conductors.

To generalize (7.6) for time-harmonic fields in a solid conductor, we integrate both sides of (4.77) over Ω_{sol} . Using the the fact that $\widehat{\Delta V}_{sol}$ is constant over Ω_{sol} , we find

$$\widehat{I}_{sol} = G_{sol} \widehat{\Delta V}_{sol} - j \omega \int_{\Omega_{sol}} \sigma \widehat{A}_z d\Omega, \quad (4.79)$$

where

$$G_{sol} = \frac{1}{\ell_z} \int_{\Omega_{sol}} \sigma d\Omega \quad (4.80)$$

is the Ohmic resistance of the solid conductor (see also e.g. [?]).

4.7.2 Stranded Conductors

The cross-section of a stranded conductor Ω_{str} is the union of several conductors, each of them too small to be modeled individually. The skin-depth is large compared to the radius of the individual conductors, allowing the skin effect in the individual conductors to be neglected. The current density \hat{J}_z is assumed to be constant over Ω_{str} . Due to magnetically induced voltages, the variation of potential drop over Ω_{str} has to be taken into account. Compared with a solid conductor, the roles of current density and voltage drop are interchanged.

While the solid conductor is a physical entity, the stranded conductor is merely a convenient mathematical tool that allows one to model, for example, the windings in the stator of an induction machine or the coil of a transformer.

Assuming that the stranded conductor is made up of N_t conductors, each carrying a current \hat{I}_{str} , the average current density is

$$\hat{J}_z = \frac{N_t \hat{I}_{str}}{S_{str}}, \quad (4.81)$$

where S_{str} is the area of Ω_{str} . The individual conductors forming the stranded conductor are assumed to be connected in series. By this assumption the potential difference $\widehat{\Delta V}_{str}$ over the latter is equal to the sum of the potential differences $\widehat{\Delta V}_{av}$ over the conductors. This sum is approximated by N_t times the average potential difference $\widehat{\Delta V}_{av}$ over an individual conductor

$$\widehat{\Delta V}_{str} = N_t \widehat{\Delta V}_{av}, \quad (4.82)$$

where

$$\widehat{\Delta V}_{av} = \frac{1}{S_{str}} \int_{\Omega_{str}} \widehat{\Delta V} d\Omega. \quad (4.83)$$

Substituting (4.78) into (4.83), taking into account that the current distribution (4.81) as well as the conductivity σ are constant over Ω , one obtains

$$\widehat{\Delta V}_{str} = R_{str} \hat{I}_{str} + j\omega \frac{N_t \ell_z}{S_{str}} \int_{\Omega_{str}} \hat{A}_z d\Omega, \quad (4.84)$$

see also e.g. [?, ?], where

$$R_{str} = \frac{N_t^2 \ell_z}{S_{str}} \int_{\Omega_{str}} \frac{1}{\sigma} d\Omega \quad (4.85)$$

is the Ohmic resistance of the stranded conductor. The insulation material surrounding the individual solid conductors and the air gaps between them can be taken into account by multiplying σ in (4.85) by a positive factor smaller than one. This factor is called the *slot fill* factor.

4.8 Induced Fields in Conductive Media

Relations (4.79) and (4.84) generalize Ohm's law (7.6) to time-harmonic currents. The first and second term of the right-hand side of (4.79) represent the resistive and inductive currents respectively. The two terms in the right-hand side of (4.84) are the resistive and inductive voltage. The relations (4.79) and (4.84) couple magnetic field quantities with integrated electric ones and are called *electrical circuit relations*.

To compute the magnetic field over the cross-section of a conductor, appropriate field equations and circuit relations have to be coupled. The right-hand side in PDE (4.75) can be written in terms of the applied voltage $\widehat{\Delta V}_{sol}$ over a solid conductor using (4.69) and (7.7)

$$\hat{J}_{s,z} = -\sigma \frac{\partial \phi}{\partial z} = \frac{\sigma}{\ell_z} \widehat{\Delta V}_{sol}, \quad (4.86)$$

and is thus constant over Ω_{sol} . It is therefore convenient to choose the PDE (4.75) in the form

$$-\frac{\partial}{\partial x} \left(\nu \frac{\partial \hat{A}_z}{\partial x} \right) - \frac{\partial}{\partial y} \left(\nu \frac{\partial \hat{A}_z}{\partial y} \right) + j\omega \sigma \hat{A}_z = \frac{\sigma}{\ell_z} \widehat{\Delta V}_{sol} \quad (4.87)$$

for the computation of the magnetic field over Ω_{sol} . By a similar argument the magnetic field over the cross-section of a stranded conductor Ω_{str} is modeled by PDE (4.74). Upon eliminating the current density by (4.81), this PDE becomes

$$-\frac{\partial}{\partial x} \left(\nu \frac{\partial \hat{A}_z}{\partial x} \right) - \frac{\partial}{\partial y} \left(\nu \frac{\partial \hat{A}_z}{\partial y} \right) = \frac{N_t}{S_{str}} \hat{I}_{str}. \quad (4.88)$$

Conductors can be excited by either a voltage or a current source. If a solid conductor is operated by a voltage source, the source term in the PDE (4.87) is a known constant, and the PDE can be solved. If instead the solid conductor is current driven, the source in the PDE has to be calculated from the electrical circuit relation (4.79). In this case, the PDE and the circuit relation have to be solved simultaneously for the magnetic vector potential and the applied voltage. To compute the magnetic field distribution of a voltage driven stranded conductor, the PDE (4.88) and the circuit relation (4.84) have to be solved simultaneously for the vector potential and the applied current.

4.9 Induced Voltage by the Time Variation of the Magnetic Flux

The voltage induced the time-varying magnetic flux is given by

$$V_{ind} = -N_t \frac{d\psi}{dt}, \quad (4.89)$$

where the minus sign is due to Lenz's Law. Using the flux-impedance relation (7.16) the above relation can be written as

$$V_{ind} = \frac{d}{dt}(LI). \quad (4.90)$$

In case that $\frac{dL}{dt} = 0$, this formula reduces to

$$V_{ind} = L \frac{d}{dt}(I). \quad (4.91)$$

The magnetic flux $\psi(t)$ passing through an oriented surface S with outward normal \mathbf{n} is given by the surface integral

$$\psi(t) = \int_S \mathbf{B} \cdot d\mathbf{S} = \int_S \mathbf{B} \cdot \mathbf{n} dS. \quad (4.92)$$

In applications of this expression we are typically interested in, the surface $S = S_{core}$ typically denotes the cross-section of the ferromagnetic core perpendicular to the flux path. In a 2D perpendicular current formulation on the domain Ω_{xy} , the surface S_{core} is then a line piece perpendicular to the y -axis extending from $x = x_m$ to $x = x_M$, extruded by a length ℓ_z in the z -direction. Using the vector potential \mathbf{A} ($\mathbf{B} = \nabla \times \mathbf{A}$) as unknown, the above expression reduces to

$$\phi(t) = \int_{S_{core}} \mathbf{B} \cdot \mathbf{n} dS \quad (4.93)$$

$$= \int_{S_{core}} B_y dx dz \quad (4.94)$$

$$= - \int_{x_m}^{x_M} dx \int_{z_m}^{z_M} dz \frac{\partial A_z}{\partial x} \quad [B_y = -\frac{\partial A_z}{\partial x}] \quad (4.95)$$

$$= -\ell_z \int_{x_m}^{x_M} dx \frac{\partial A_z}{\partial x} \quad (4.96)$$

$$= -\ell_z [A_z(x = x_M, t) - A_z(x = x_m, t)] \quad (4.97)$$

$$= \ell_z [A_z(x = x_m, t) - A_z(x = x_M, t)]. \quad (4.98)$$

In other applications S might consist of a component S_{core} in the core and a component S_{air} in air (refer to the open core FCL). In this we can write

$$\phi^{tot}(t) = \phi^{core}(t) + \phi^{air}(t) \approx \phi^{core}(t) \quad \text{if} \quad \phi^{air}(t) \text{ is small.} \quad (4.99)$$

In an azimuthal current application we have that ...

4.10 Induced Voltage by a Homogenization Procedure

In this section we review a technique allowing to compute the induced voltage in winded coils (also referred to as *stranded conductors*) by integrating its density over the volume in 3D (cross-section in 2D) of the conductor.

4.10.1 Three Dimensional

Need to include pictures of the 3D coils

To compute the induced voltage in winded coils the introduction of the so-called *winding function* t turns out to be useful. This is a vector function such that the applied current density in the coil can be expressed as

$$\mathbf{J} = I \mathbf{t} \quad (4.100)$$

We next give two examples of winding functions. For a *cylindrical coil* in the xy -plane with center in (x_0, y_0, z_0) , cross-section S and number of turns N_t and excited by a current flowing in counter clock wise direction, we have that $\mathbf{t}(x, y, z) = \frac{N_t}{S}(t_x(x, y), t_y(x, y), 0)$ where

$$t_x(x, y) = \frac{-(y - y_0)}{\sqrt{(x - x_0)^2 + (y - y_0)^2}} \text{ and } t_y(x, y) = \frac{x - x_0}{\sqrt{(x - x_0)^2 + (y - y_0)^2}}. \quad (4.101)$$

For a *cuboidal coil* occupying the surface $\Omega = (x_0, y_0) + ([-D, D] \times [-W, W] \setminus [-d, d] \times [-w, w])$ in the xy -plane extruded in the z -direction excited by a current in counter clockwise direction, we have again that $\mathbf{t}(x, y, z) = \frac{N_t}{S}(t_x(x, y), t_y(x, y), 0)$ where

$$t_x(x, y) = \begin{cases} -\text{sgn}(y) & \text{if } |y - y_0| > \frac{w}{d}|x - x_0| \\ 0 & \text{otherwise} \end{cases} \text{ and } t_y(x, y) = \begin{cases} \text{sgn}(x) & \text{if } |y - y_0| \leq \frac{w}{d}|x - x_0| \\ 0 & \text{otherwise} \end{cases}. \quad (4.102)$$

In both cases we have that

$$\nabla \cdot \mathbf{t} = 0 \text{ (and thus } \nabla \cdot \mathbf{J} = 0) \text{ and } \|\mathbf{t}\| = \frac{N_t}{S}. \quad (4.103)$$

By a homogenization procedure over the individual windings in the coil, the induced voltage can be computed by integrating the density defined by the dot product $\mathbf{t} \cdot \mathbf{E}$ over the volume of the coil

$$V_{ind} = \int_{\Omega_{coil}} \mathbf{t} \cdot \mathbf{E} d\Omega. \quad (4.104)$$

Combining with the previous result, we have that

$$\boxed{\frac{d}{dt}(LI) = -N_t \frac{d\psi(t)}{dt} = \int_{\Omega_{coil}} \mathbf{t} \cdot \mathbf{E} d\Omega.} \quad (4.105)$$

This relation is the basis for the field-circuit coupling modeling of a winded coil excited by a voltage source. In what follows we make the relation for the induced voltage more explicit in two-dimensional computations.

4.10.2 Two Dimensional Perpendicular Current

In a perpendicular current computation we assume the cross-section of a winded coil to consist of components $S_{coil,1}$ and $S_{coil,2}$, excited by a current in positive and negative z -direction, respectively. The induced can then be computed as as follows

$$V_{ind} = V_{ind,1} + V_{ind,2} \quad (4.106)$$

$$= \frac{N_t \ell_z}{S_{coil,1}} \int_{S_{coil,1}} E_z dS - \frac{N_t \ell_z}{S_{coil,2}} \int_{S_{coil,2}} E_z dS \quad (4.107)$$

$$= \frac{N_t \ell_z}{S_{coil,1}} \int_{S_{coil,1}} \frac{\partial A_z}{\partial t} dS - \frac{N_t \ell_z}{S_{coil,2}} \int_{S_{coil,2}} \frac{\partial A_z}{\partial t} dS \quad (4.108)$$

where the minus sign stems from the fact that the current flows in opposite directions in both sides of the coil.

4.10.3 Two Dimensional Azimuthal Current

In a azimuthal current computation we the induced voltage in a coil with cross-section S_{coil} can be expressed as

$$V_{ind} = \frac{N_t}{S_{coil}} \int_{S_{coil}} 2\pi r E_\phi dS \quad (4.109)$$

$$= \frac{N_t}{S_{coil}} \int_{S_{coil}} 2\pi r \frac{\partial A_\phi}{\partial t} dS \quad (4.110)$$

4.11 Boundary Conditions

The partial differential equations introduced before need to be supplied with boundary conditions. In this work we will make use of homogeneous Dirichlet, Neumann and periodic boundary conditions. When used in combination with a conformal mapping technique, the latter allow the modeling of infinite domains.

4.11.1 Axial Symmetry

4.11.2 Symmetry Boundary Conditions

4.11.3 Periodic Boundary Conditions

Let Γ_1 and Γ_2 be two disjoint parts of the boundary of the computational domain as shown in Figure ?? on page ?? for example. Let n_1 and n_2 denote the outward normal on Γ_1 and Γ_2 respectively. Periodic boundary conditions connect both the vector potential and its normal derivative on Γ_1 and Γ_2 . Periodic boundary conditions state that

$$A_z|_{\Gamma_1} = A_z|_{\Gamma_2} \quad (4.111)$$

$$\nu \frac{\partial A_z}{\partial n_1}|_{\Gamma_1} = -\nu \frac{\partial A_z}{\partial n_2}|_{\Gamma_2}. \quad (4.112)$$

Anti-periodic boundary conditions state that

$$A_z|_{\Gamma_1} = -A_z|_{\Gamma_2} \quad (4.113)$$

$$\nu \frac{\partial A_z}{\partial n_1}|_{\Gamma_1} = \nu \frac{\partial A_z}{\partial n_2}|_{\Gamma_2} \quad (4.114)$$

see e.g. [2, ?]. By imposing periodic boundary conditions one is able to reduce the area of the computational domain. We illustrate this point by an example. Consider the four-pole alternating current machine depicted in Figure ?? on page ?. Due to symmetry in field and geometry, it is sufficient to model only two, or even just one pole of the machine. Figure ?? shows a two-pole half model of the motor being considered. In this model periodic boundary conditions relate the values on the straight edges at the bottom of the model. In the one-pole quarter model shown in Figure ??, anti-periodic boundary conditions relate the values of the vertical and horizontal straight edge.

The reduction of the computational domain entails a saving in computational resources required to solve the problem or allows to obtain higher accuracy for the same problem size.

4.11.4 Unbounded Domains

In some practical magnetic field computations the domain Ω is unbounded. Different types of so-called *open boundary problems* exist. In a first one the accurate estimation of the field in a region of interest might require taking the surrounding unbounded domain into account. In a second type one is interested in far field effects, i.e. in the strength of the field at a large distance from the source. An example of the former is the computation of the magnetic field in the vicinity of a transformer. An example of the latter is the computation of the magnetic field excited by high voltage lines at ground level.

In numerical computations the unbounded domain needs to be truncated somehow. An overview of truncation techniques proposed in the literature can be found in [?].

In the application software considered in this work, a conformal mapping technique is used. To describe this technique formally, consider equation (4.47) posed on the domain $\Omega = \mathbb{R}^2$. The PDE has to be supplied with the condition that the potential remains finite at infinity. By properly scaling the potential, one can assume the value at infinity to be zero, i.e.

$$A_z(x, y) \rightarrow 0 \quad \text{as } \sqrt{x^2 + y^2} \rightarrow \infty. \quad (4.115)$$

The part of Ω that is of interest is enclosed in a disk Ω_D centered in $(0, 0)$. The radius ρ of Ω_D is required to be large enough so that the source term J_z is zero on $(\Omega_D)^c = \mathbb{R}^2 \setminus \Omega_D$. We further assume ν to be constant on $(\Omega_D)^c$. Hence, the function A_z satisfies the Laplace equation on $(\Omega_D)^c$. Let A_D and A_{D^c} denote the restriction of A_z to Ω_D and $(\Omega_D)^c$ and n_D and n_{D^c} the outward normal on Ω_D and $(\Omega_D)^c$ respectively. The original problem on \mathbb{R}^2 is equivalent with

$$\begin{aligned} -\frac{\partial}{\partial x} \left(\nu \frac{\partial A_D}{\partial x} \right) - \frac{\partial}{\partial y} \left(\nu \frac{\partial A_D}{\partial y} \right) &= J_z & \text{on } \Omega_D \\ -\frac{\partial^2 A_{D^c}}{\partial x^2} - \frac{\partial^2 A_{D^c}}{\partial y^2} &= 0 & \text{on } (\Omega_D)^c, \end{aligned} \quad (4.116)$$

supplied with conditions ensuring the continuity of A_z and its normal flux across the boundary $\partial\Omega_D$. These continuity conditions can be stated as

$$A_D|_{\partial\Omega_D} = A_{D^c}|_{\partial\Omega_D} \quad \text{and} \quad \nu \frac{\partial A_D}{\partial n_D}|_{\partial\Omega_D} = -\nu \frac{\partial A_{D^c}}{\partial n_{D^c}}|_{\partial\Omega_D}. \quad (4.117)$$

After setting $z = x + jy$, one applies the conformal mapping

$$\mathcal{F}(z) = 1/z \quad (4.118)$$

to $(\Omega_D)^c$. The latter is mapped onto a disk Ω_E with radius $1/\rho$

$$\mathcal{F}[(\Omega_D)^c] = \Omega_E. \quad (4.119)$$

Properties of conformal transformations imply that the function A_{D^c} is a harmonic function on the image disk Ω_E if A_{D^c} is harmonic on the domain $(\Omega_D)^c$. The conformal mapping thus transforms the differential problem (4.116)-(4.117) into

$$\begin{aligned} -\frac{\partial}{\partial x} \left(\nu \frac{\partial A_D}{\partial x} \right) - \frac{\partial}{\partial y} \left(\nu \frac{\partial A_D}{\partial y} \right) &= J_z & \text{on } \Omega_D \\ -\frac{\partial^2 A_{D^c}}{\partial x^2} - \frac{\partial^2 A_{D^c}}{\partial y^2} &= 0 & \text{on } \Omega_E \end{aligned} \quad (4.120)$$

supplied with the conditions

$$A_D|_{\partial\Omega_D} = A_{D^c}|_{\partial\Omega_E} \quad \text{and} \quad \nu \frac{\partial A_D}{\partial n_D}|_{\partial\Omega_D} = -\rho^2 \nu \frac{\partial A_{D^c}}{\partial n_E}|_{\partial\Omega_E}, \quad (4.121)$$

where n_E denotes the outward normal on Ω_E . The factor ρ^2 appearing in (4.121) is due to the local magnification $1/|\mathcal{F}'|$ evaluated on $\partial\Omega_D$ by conformal mapping. Using a conformal mapping we have thus transformed the original unbounded domain problem into two problems on bounded domains: a Poisson type problem on Ω_D and a Laplace problem on Ω_E . The condition (4.115) is assured by imposing the potential to be zero in the center of Ω_E

$$A_z = 0 \quad \text{in center of } \Omega_E. \quad (4.122)$$

Chapter 5

Magnetic Saturation

In this section we describe the modeling of magnetic saturation in ferromagnetic materials, i.e., the modeling of the non-linear constitutive relation between the magnetic flux \mathbf{B} (units T) and the magnetic field \mathbf{H} (units A/m). Using a vector potential formulation and denoting by $B = \|\mathbf{B}\|$, $H = \|\mathbf{H}\|$, the magnetic material law typically considered is

$$H(B) = \nu B = \nu_0 \nu_r(B) B \Leftrightarrow \nu(B) = \frac{dH}{dB}(B), \quad (5.1)$$

where ν_0 and ν (ν_r) denote the reluctivity of vacuum and the material (relative reluctivity), respectively [see paper Herbert on differential vs. chord reluctivity]. The inverse of the reluctivity is the permeability μ . Using a vector potential formulation, we have that

$$\|B\|^2 = \left(\frac{\partial A_z}{\partial y} - \frac{\partial A_y}{\partial z} \right)^2 + \left(-\frac{\partial A_z}{\partial x} + \frac{\partial A_x}{\partial z} \right)^2 + \left(\frac{\partial A_y}{\partial x} - \frac{\partial A_x}{\partial y} \right)^2 \quad (5.2)$$

Magnetic saturation is such that $\mu_r(B)$ is large and almost constant for small values of B and small almost constant for large values of B and has a non-linear transition between these two extreme values (see for instance Figure xxx).

In practise engineering practise, the function $\nu_r(B)$ is to be constructed from measured B - H samples. This process makes the convergence of an FEM computation prone stagnation. We therefore consider analytical expressions allowing to describe the function $\nu_r(B)$ analytically.

Goals In this chapter we aim at

- giving different analytical expressions for the non-linear B - H -curve modelling magnetic saturation
- give an example of a measured B - H
- illustrate a least square curve fitting technique allow to match the analytical expressions to the given measured data

To do

- add reference to rational BH-curve approximation
- add reference to Pechstein on approximating the BH-curve

5.1 Analytical Models

To do:

- make all plots of the BH-curves again

- compute the second derivative of the analytical model to see where the curvature changes from positive to negative.
- give a plot on double axis and deduce for which value of the current the core is in saturation.

5.1.1 Rational Function Approximation

In [?] the following rational expression modelling the relative reluctivity is given (denoting by $B = \|\mathbf{B}\|$)

$$\nu_r = a + \frac{(1-a)B^{2b}}{B^{2b} + c} \Leftrightarrow \mu_r = \frac{1}{a + \frac{(1-a)B^{2b}}{B^{2b} + c}} \quad (5.3)$$

where the values for the parameters a , b and c are given in Table 5.1. For this models holds that

$$\nu_r(B = 0) = a \quad (5.4)$$

and thus the relative permeability at $B = 0$ is given by $1/a$ and that

$$\lim_{B \rightarrow \infty} \nu_r(B) = 1 \quad (5.5)$$

and thus the permeability never becomes smaller than μ_0 (which is physically correct).

a	2.12e-4
b	7.358
c	1.18e6

Table 5.1: Constants Used in the Rational Approximation

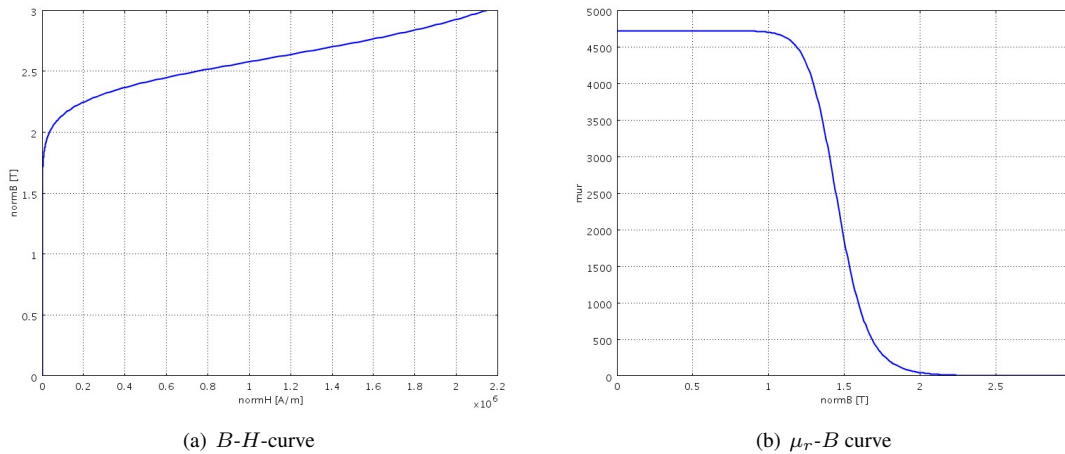


Figure 5.1: Rational Function Approximation of the B - H curve.

5.1.2 Hyperbolic Function Approximation

In [?] the following approximation is given:

$$B = C_1 \operatorname{arcsinh}(C_2 H) \Leftrightarrow H = \frac{1}{C_2} \sinh\left(\frac{B}{C_1}\right) \quad (5.6)$$

where the values for the parameters C_1 and C_2 are given in Table (5.2). From this we obtain the chord permeability

$$\mu = \frac{B}{H} = \frac{C_2 B}{\sinh(\frac{B}{C_1})} \tag{5.7}$$

$$\mu_r = \frac{\mu}{\mu_0} = \frac{C_2 B}{\mu_0 \sinh(\frac{B}{C_1})} \tag{5.8}$$

and the differential permeability

$$\nu = \frac{dH}{dB} = \frac{\cosh(C_2 B)}{C_1 C_2} \tag{5.9}$$

$$\mu = \frac{1}{\nu} = \frac{C_1 C_2}{\cosh(C_2 B)} \tag{5.10}$$

$$\mu_r = \frac{\mu}{\mu_0} = \frac{C_1 C_2}{\mu_0 \cosh(C_2 B)} \tag{5.11}$$

$$\tag{5.12}$$

As in this model

$$\lim_{B2 \rightarrow \infty} \mu_r(B2) = 0, \tag{5.13}$$

is has to be used with due care.

Remark This model requires a non-zero initial guess during intial guess to avoid the singularity at $B = 0$.

C_1	.25 [T]
C_2	.06 [m/A]

Table 5.2: Constants Used in the Sinh Approximation

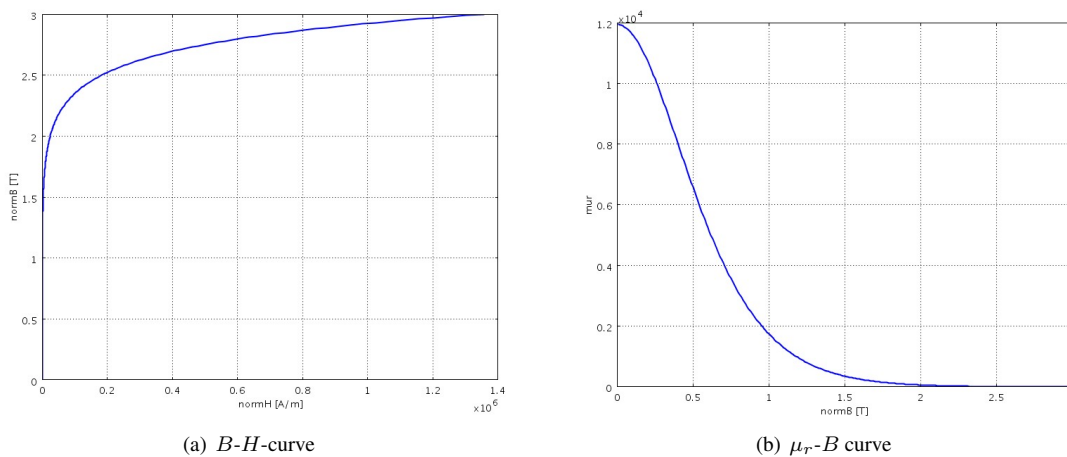


Figure 5.2: Hyperbolic Function Approximation of a $B-H$ curve.

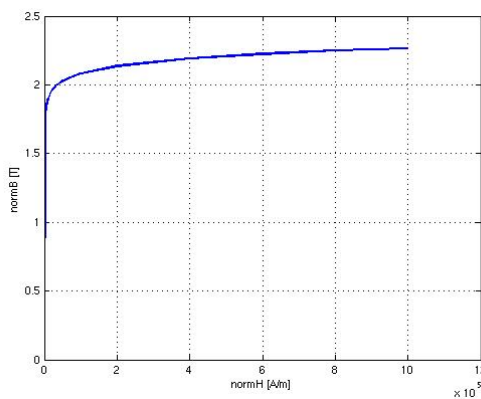
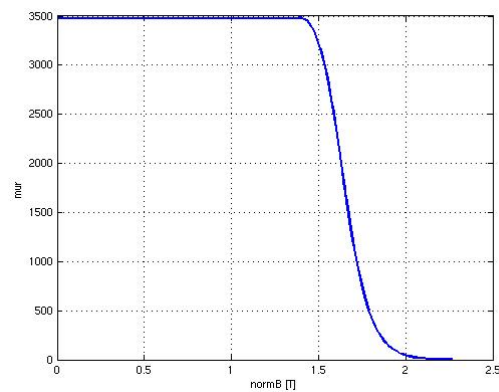
5.2 Measured Data

In this section we give the measured $B-H$ -data we will use in our numerical examples in subsequent chapters.

5.2.1 Measured BH data

```
H = [0 310      315      320      330      350      380      410      430 ...
470      500      540      580      620      650      670      720      750 ...
770      820      900      1000     1100     1200     1400     1800     2300 ...
2800     3300     4300     5300     8300     10300    15300    20300    25300 ...
30300    40300    50300    70300    100300   200300   400300   600300   800300 ...
1000300];
```

```
B = [0 1.3449    1.3773    1.4003    1.4328    1.4736    1.5112    1.5367    1.5501 ...
1.5715    1.5845    1.5991    1.6114    1.6221    1.6293    1.6337    1.6439    1.6494 ...
1.6529    1.661      1.6724    1.6847    1.6954    1.7048    1.7209    1.7457 ...
1.7687    1.7866    1.8012    1.8242    1.842     1.8796    1.8975    1.9299    1.9529 ...
1.9708    1.9854    2.0084    2.0262    2.0532    2.0817    2.1371    2.1926    2.225 ...
2.248     2.2659 ];
```

(a) B - H -curve(b) μ_r - B curveFigure 5.3: B - H -curve used in tabular form.

5.3 Tuning the Analytical Models

In this section we perform a fitting of the parameters in the rational and hyperbolic approximation to the measured data by a non-linear optimisation procedure.

5.4 Further Extension

1. Make graphs of the derivative of μ_r wrt normB for the analytical and tabular data models. These graphs should show how the tabular is more difficult to work with.

Chapter 6

Magnetic Force Computation Methods

In this section we recall three classical methods for computing the magnetic force: the Lorentz method, the Maxwell Stress Tensor method and the Virtual Work method.

6.0.1 Lorentz Method

In Lorentz method the total magnetic force \mathbf{F} on a current carrying device is computed by integrating the volume force density $\mathbf{J} \times \mathbf{B}$ over the volume V of the device

$$\mathbf{F} = \int_V \mathbf{J} \times \mathbf{B} dV. \quad (6.1)$$

In 2D perpendicular current computations the domain of integration reduces to a cross section which we denote by Ω_1 . Substituting (4.39) and (4.41) for \mathbf{J} and \mathbf{B} into (6.1) we obtain for the x - and y -components of the total force

$$F_x = - \int_{\Omega_1} J_z B_y d\Omega_1 \text{ and } F_y = \int_{\Omega_1} J_z B_x d\Omega_1. \quad (6.2)$$

Remark 6.0.1 *Lorentz method can only be applied to electrical conductors with $\mu_r = 1$. The method does not allow computing the force on permanent magnets.*

6.0.2 Maxwell Stress Tensor Method

In the Maxwell Stress Tensor (MST) method the total force on a magnetizable device with unit outward normal \mathbf{n} on its enclosing surface S is computed by integrating the product of the Maxwell stress tensor σ_{EM} and \mathbf{n} over the enclosing surface

$$\mathbf{F} = \int_S \sigma_{EM} \mathbf{n} dS. \quad (6.3)$$

In this paper we always assume that the device on which we want to compute the force is surrounded by empty space. Then the Maxwell stress tensor is given by

$$\sigma_{EM} = -\frac{1}{2\mu_0} (\mathbf{B} \cdot \mathbf{B}) I + \frac{1}{\mu_0} \mathbf{B} \mathbf{B}^T, \quad (6.4)$$

where I denotes the identity matrix.

In 2D perpendicular current computations the stress tensor simplifies to the 2×2 matrix

$$\sigma_{EM} = -\frac{1}{2\mu_0} \begin{pmatrix} B_x^2 + B_y^2 & 0 \\ 0 & B_x^2 + B_y^2 \end{pmatrix} + \frac{1}{\mu_0} \begin{pmatrix} B_x^2 & B_x B_y \\ B_x B_y & B_y^2 \end{pmatrix}, \quad (6.5)$$

while the domain of integration in (6.3) reduces to the boundary of the 2D cross section of the device denoted by Γ_1 . By substituting

$$H_x = \nu_0 B_x \text{ and } H_y = \nu_0 B_y \quad (6.6)$$

in (6.5) we obtain the following expressions for the x - and y -components of the total force

$$F_x = \int_{\Gamma_1} \left[-\frac{1}{2} n_x (H_x B_x + H_y B_y) + B_x (n_x H_x + n_y H_y) \right] d\Gamma_1, \quad (6.7)$$

and

$$F_y = \int_{\Gamma_1} \left[-\frac{1}{2} n_y (H_x B_x + H_y B_y) + B_y (n_x H_x + n_y H_y) \right] d\Gamma_1. \quad (6.8)$$

6.0.3 Virtual Work Method

In the Virtual Work method the force is computed from the magnetic energy of the system. The magnetic energy W_{EM} of a system with volume V is given by

$$W_{EM} = \int_V \left(\int_0^B \mathbf{H} \cdot d\mathbf{B} \right). \quad (6.9)$$

Under constant magnetic flux condition, the magnetic force is computed as

$$\mathbf{F}_\Phi = -\nabla W_{EM}. \quad (6.10)$$

Under constant current condition, the force is computed similarly, but with opposite sign.

Chapter 7

Lumped Parameter Models of RL Circuits

Prior to detailing finite element models in subsequent chapters, we develop in this chapter simplified lumped parameter approximation that serve to get an intuitive feeling and point of comparison for the subsequent models. The point of departure for deriving lumped parameter models is the following first order ordinary differential equation relating the externally applied voltage excitation $V_e(t)$ with the current $I(t)$ in a circuit with an Ohmic resistance R and inductance L .

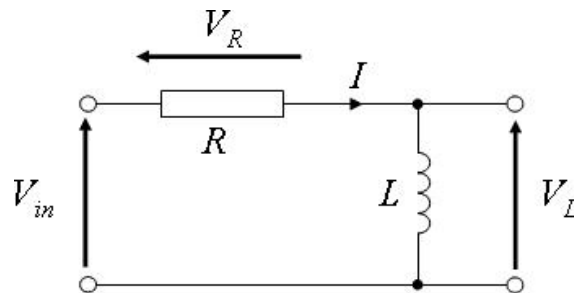


Figure 7.1: Series connection of a resistance and inductance.

$$V_R(t) + V_L(t) = V_{in}(t) \Leftrightarrow \frac{d}{dt}(LI) + RI = V_e(t). \quad (7.1)$$

The terms in the left-hand side can be identified as the induced and resistive voltage, respectively, and the equation states that at all times the sum of the induced and resistive voltage is equal to the externally applied one. The equation needs to be supplied with an initial value for the current.

The Ohmic resistance R determined by the electrical conductivity of the medium. In the case that the coil is solenoid wounded N_t times around a ferromagnetic core with magnetic permeability μ , the impedance L can be expressed as

$$L = \mu N_t^2 \frac{S}{l_{path}} = \mu_0 \mu_r N_t^2 \frac{S}{l_{path}}, \quad (7.2)$$

where S and l_{path} cross-section and length of the flux path in the ferromagnetic core respectively.

In this chapter we first derive an analytical expression for the current in an RL-circuit with *constant* impedance and two excitations: a constant and sinusoidally varying voltage source. These models illustrate how the presence of an impedance causes a phase shift in and amplitude reduction of the current. In more realistic models however the magnetic permeability μ of the core changes by moving the operation point on a non-linear B - H characteristic. In a second stage we therefore extend the model to include *changes* in the impedance induced by changes in the magnetic permeability. This model assumes the coil to be a solenoid for which expression (7.2) is correct. The generalisation of this model to more complex coil-core configurations is therefore not immediate.

Describe a mechanical equivalent: variable impedance and variable mass.

Goals In this chapter we aim at

- describing a simple model able to explain the inductive current limiting principle (including the concepts of induced voltage and phase difference between applied voltage and current). This simple model can possibly serve as coarse model inside an surrogate based optimisation algorithm.
- explaining why this simple model is not sufficient for the type of devices considered

To do:

1. describe drop in resistive voltage
2. describe presence of DC coil by additive constant in the flux

7.1 Ohmic Resistance of a Wire

Consider a cylindrical electrical conductor along the z -axis with length ℓ_z and cross-section Ω in the xy plane. The shape of the cross-section Ω is assumed to be z -independent. Consider furthermore a *stationary* electrical current flowing along the z -axis through the conductor. For stationary fields Faraday's law implies that the electric field \mathbf{E} is curl free. This condition can be ensured by writing \mathbf{E} in terms of the electric potential ϕ as

$$\mathbf{E} = -\nabla\phi. \quad (7.3)$$

Substituting this into Ohm's law $\mathbf{E} = \sigma \mathbf{J}$ yields

$$\mathbf{J} = -\sigma \nabla\phi. \quad (7.4)$$

For currents flowing in the z -direction only, the above relation yields

$$J_z = -\sigma \frac{\partial\phi}{\partial z}. \quad (7.5)$$

Assuming the gradient $\partial\phi/\partial z$ to be constant over the cross-section Ω , we obtain Ohm's law by integrating (7.5) over Ω in integral form

$$\Delta V = R I, \quad (7.6)$$

where

$$\Delta V = -\ell_z \frac{\partial\phi}{\partial z} \quad (7.7)$$

and

$$I = \int_{\Omega} J_z d\Omega \quad (7.8)$$

are the voltage drop over and the current through the conductor and where

$$R = \ell_z / \left(\int_{\Omega} \sigma d\Omega \right) \quad (7.9)$$

is the ohmic resistance of the conductor expressed in Ohm Ω . Equation (7.6) can be rewritten as

$$I = G \Delta V, \quad (7.10)$$

where

$$G = \frac{1}{R}, \quad (7.11)$$

is the conductance of the conductor.

7.2 Inductance of a Winded Coils

7.2.1 Definition

- give definition of (self and mutual) inductance
- give units (Henry) and function of primary units

$$1\text{H} = 1\text{Wb}/\text{A} = 1\text{T m}^2/\text{A} = 1 \frac{\text{Vs}}{\text{m}^2} \text{m}^2/\text{A} = 1 \frac{\text{V}}{\text{A}} \text{s} = 1\Omega \text{s} \quad (7.12)$$

- give range of value for applications (tens of miliHenry)

7.2.2 Magnetic Energy

Consider that the volume Ω encloses the core and ferromagnetic core and has a permeability $\mu = \mu(\mathbf{x}, t)$. The magnetic energy W_m in Ω due to the magnetic flux \mathbf{B} and field \mathbf{H} induced due a time-varying current is given by the volume integral

$$W_m(t) = \frac{1}{2} \int_{\Omega} \mathbf{B} \cdot \mathbf{H} d\Omega = \frac{1}{2} \int_{\Omega} \mu \mathbf{B} \cdot \mathbf{B} d\Omega. \quad (7.13)$$

In a 2D perpendicular current formulation on a computational domain with cross-section Ω_{xy} in the xy -plane and length ℓ_z in the z -direction (examples will be given in subsequent chapters), this formula simplifies to the surface integral

$$W_m(t) = \frac{\ell_z}{2} \int_{\Omega_{xy}} [B_x H_x + B_y H_y] d\Omega = \frac{\ell_z}{2} \int_{\Omega_{xy}} \mu [B_x B_x + B_y B_y] d\Omega. \quad (7.14)$$

In case that the magnetic field is generated by a total current $I_{tot}(t)$ flowing through a coil with N_t windings and current $I(t)$ per turn, i.e., $I_{tot}(t) = N_t I(t)$, the magnetic energy and the coil impedance $L(t)$ are related by

$$W_m(t) = \frac{1}{2} L(t) I^2(t) \Leftrightarrow L(t) = 2 \frac{W_m(t)}{I^2(t)}. \quad (7.15)$$

Not that the inductance scales

- *quadratically* with N_t ;
- *linearly* with μ .

In case that μ is constant (no magnetic saturation), the impedance is current independent and can therefore be computed using any non-zero value for the current. In case that a sinusoidal current brings (a part of) the core alternatively in and out of saturation, the impedance can be computed for a particular working condition. In configurations in which different coils are present (AC and DC coil in the fault current limiter), the self-inductance of the coil can be computed by considering the current in the single coil only (setting the current in the other coils equal to zero).

7.2.3 Magnetic Flux

Considering the coil to be an interconnection of N_t flux contributions, the magnetic flux and the coil impedance are related by

$$\psi(t) = N_t \phi(t) = L(t) I(t) \Leftrightarrow L(t) = \frac{N_t \psi(t)}{I(t)} = \frac{\phi(t)}{I(t)}. \quad (7.16)$$

Assuming that $I(t) \neq 0$, this expression allow to compute the impedance via the magnetic flux.

7.3 Impedance

The Ohmic resistance of the wire and the inductance of a coil can be combined to form the total impedance denoted by X and defined by

$$X = \sqrt{R^2 + \omega^2 L^2}. \quad (7.17)$$

7.4 Constant Inductance Model

In this section we assume that $\frac{dL}{dt} = 0$. In this case, equation (7.1) reduces to

$$L \frac{dI}{dt} + RI = V(t). \quad (7.18)$$

Given some initial condition, this ordinary differential equation can be solved numerically using a time-integrator taking a time-dependent resistance (simulation of fault) into account. In order to derive analytical expressions however, we assume from here on that $\frac{dR}{dt} = 0$. The ratio $\frac{R}{L}$ has the dimensions of an (angular) pulsation and will be denoted by ω_1 from here on. The solution of the homogeneous equation to (7.18) is

$$I_h(t) = C \exp(-R/Lt) = C \exp(-\omega_1 t) \quad (7.19)$$

where C is chosen so to satisfy the initial conditions.

7.4.1 Constant Applied Voltage

In case that the applied voltage is constant and equal to V_0 , the method of variation of constants yields that $I(t) = C(t) I_h(t)$, where

$$C'(t) = V_0/L \exp(\omega_1 t) \Rightarrow C(t) = V_0/L \omega_1 \exp(\omega_1 t) + C_0 = V_0/R \exp(\omega_1 t) + C_0. \quad (7.20)$$

For the current we then have

$$I(t) = [V_0/R \exp(\omega_1 t) + C_0] \exp(-\omega_1 t) \quad (7.21)$$

$$= V_0/R + C_0 \exp(-\omega_1 t), \quad (7.22)$$

where the integration constant C_0 is related to the initial condition $I(t=0) = I_0$ by

$$C_0 = I_0 - V_0/R. \quad (7.23)$$

The current is then given by

$$I(t) = \frac{V_0}{R} + [I_0 - V_0/R] \exp(-\omega_1 t). \quad (7.24)$$

If the relaxation time $\tau = L/R$ is sufficiently small (i.e., if the resistance R is not too small and the inductance L is not too large), then after a few multiples of the relaxation time, the current is independent of the initial condition and equal to its stationary value

$$\boxed{I(t) = \frac{V_0}{R}}. \quad (7.25)$$

7.4.2 Sinusoidally Varying Applied Voltage

In case that the applied is sinusoidally varying, i.e., $V(t) = V_0 \sin(\omega_0 t)$, the method of variation of constants yields that $I(t) = C(t) I_h(t)$, where

$$C'(t) = V_0/L \sin(\omega_0 t) \exp(\omega_1 t) \Rightarrow C(t) = (V_0/L) \int^t \sin(\omega_0 s) \exp(\omega_1 s) ds + C_0. \quad (7.26)$$

for some integration constant C_0 . Applying integration by parts twice yields

$$L/V_0 C(t) = [1/\omega_1 \sin(\omega_0 s) \exp(\omega_1 s)]^t - \omega_0/\omega_1 \int^t \cos(\omega_0 t) \exp(\omega_1 s) ds + C_0 \quad (7.27)$$

$$= 1/\omega_1 \sin(\omega_0 t) \exp(\omega_1 t) - \omega_0/\omega_1^2 [\cos(\omega_0 s) \exp(\omega_1 s)]^t \quad (7.28)$$

$$- \omega_0^2/\omega_1^2 \int^t \sin(\omega_0 s) \exp(\omega_1 s) ds + C_0 \quad (7.29)$$

$$= 1/\omega_1 \sin(\omega_0 t) \exp(\omega_1 t) - \omega_0/\omega_1^2 \cos(\omega_0 t) \exp(\omega_1 t) \quad (7.30)$$

$$- \omega_0^2/\omega_1^2 \int^t \sin(\omega_0 s) \exp(\omega_1 s) ds + C_0 \quad (7.31)$$

Hence

$$[1 + \omega_0^2/\omega_1^2] C(t) = 1/\omega_1 (V_0/L) \sin(\omega_0 t) \exp(\omega_1 t) - \omega_0/\omega_1^2 (V_0/L) \cos(\omega_0 t) \exp(\omega_1 t) + C_0 \quad (7.32)$$

or

$$C(t) = (V_0/L) \left[\frac{\omega_1}{\omega_0^2 + \omega_1^2} \sin(\omega_0 t) - \frac{\omega_0}{\omega_0^2 + \omega_1^2} \cos(\omega_0 t) \right] \exp(\omega_1 t) + C_0 \quad (7.33)$$

$$= \frac{V_0}{L(\omega_0^2 + \omega_1^2)} [\omega_1 \sin(\omega_0 t) - \omega_0 \cos(\omega_0 t)] \exp(\omega_1 t) + C_0 \quad (7.34)$$

$$= \frac{V_0 \sqrt{\omega_0^2 + \omega_1^2}}{L(\omega_0^2 + \omega_1^2)} \left[\frac{\omega_1}{\sqrt{\omega_0^2 + \omega_1^2}} \sin(\omega_0 t) - \frac{\omega_0}{\sqrt{\omega_0^2 + \omega_1^2}} \cos(\omega_0 t) \right] \exp(\omega_1 t) + C_0 \quad (7.35)$$

$$= \frac{V_0}{L \sqrt{\omega_0^2 + \omega_1^2}} [\sin(\omega_0 t) \cos \Theta - \cos(\omega_0 t) \sin \Theta] \exp(\omega_1 t) + C_0 \quad (7.36)$$

$$= \frac{V_0}{X} \sin(\omega_0 t - \Theta) \exp(\omega_1 t) + C_0 \quad (7.37)$$

where we've introduced the phase shift

$$\frac{\sin \Theta}{\cos \Theta} = \frac{\omega_0}{\omega_1} \Leftrightarrow \Theta = \arctan\left(\frac{\omega_0}{\omega_1}\right) = \arctan\left(\frac{2\pi f R}{L}\right), \quad (7.38)$$

and where the integration constant C_0 is related to the initial condition by

$$C_0 = I_0 - \frac{V_0}{X} \sin(\Theta). \quad (7.39)$$

The current is then given by

$$I(t) = \frac{V_0}{X} \sin(\omega_0 t - \Theta) + \left[I_0 - \frac{V_0}{X} \sin \Theta \right] \exp(-\omega_1 t). \quad (7.40)$$

If the relaxation time $\tau = 1/\omega_1 = L/R$ is sufficiently large, then after a few multiples of the relaxation time, the current is independent of the initial condition and equal to

$$\boxed{I(t) = \frac{V_0}{X} \sin(\omega_0 t - \Theta)}. \quad (7.41)$$

Compared with a purely resistive network, the current has both a lower amplitude and a phase shift. A large inductance in particular will lead to a lower current value and a larger phase shift. This is illustrated in Figure 7.4.2.

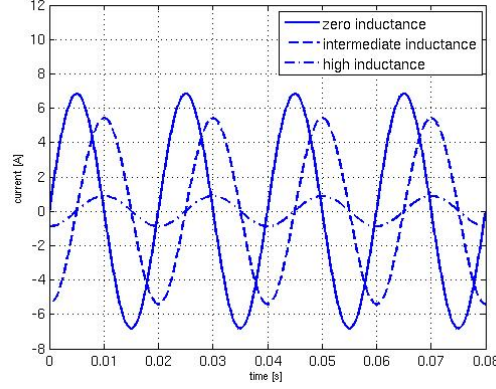


Figure 7.2: Current in RL-circuit for different values of the inductance.

7.5 Flux-Variable Inductance Model

The models developed in the previous section cease to be valid in situations in which the working point changes in time over a range in which the permeability and therefore the impedance can no longer assumed to be constant. The case that we will be interested in is the one in which the permeability varies along a non-linear B - H characteristic and which time-varying voltage source bringing the ferromagnetic core in (low permeability and impedance) and out (high permeability and impedance) of saturation.

To extend our models to variable impedance cases, it turns out to be convenient to replace the current by the flux as state variable

$$\psi = L I \Leftrightarrow I = \frac{\psi}{L(\psi)} \quad (7.42)$$

and to rewrite the equation (7.1) modelling an RL-circuit as

$$\frac{d}{dt}\psi + \frac{R}{L(\psi)}\psi = V(t). \quad (7.43)$$

In this model the variable impedance can be computed using the non-linear characteristic data assuming the model (7.2) for a solenoid. In this case we have that

$$L(\psi) = \mu[B(\psi)]N_t^2 \frac{S}{l_{path}} \quad (7.44)$$

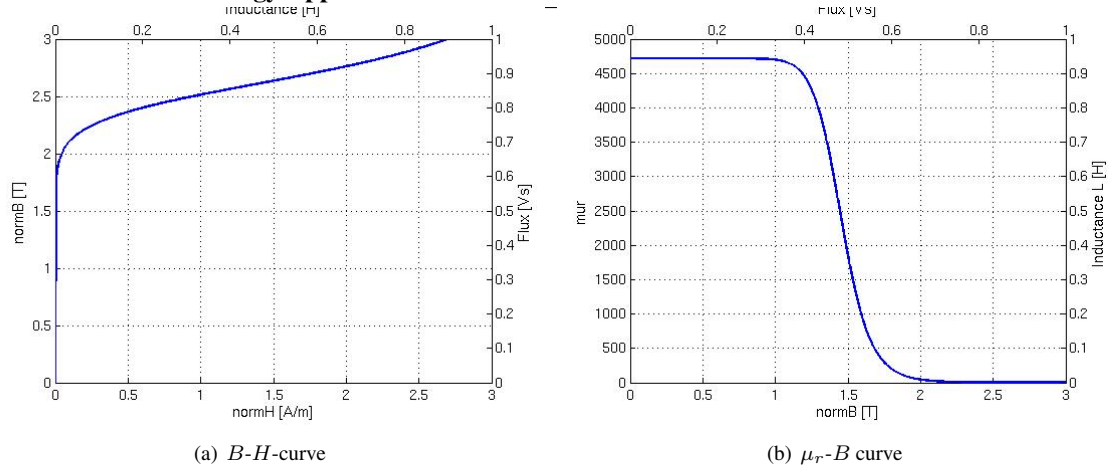
$$= \mu\left[\frac{\psi}{S}\right]N_t^2 \frac{S}{l_{path}}. \quad (7.45)$$

Given an initial condition $\psi(t=0) = L(t=0)I(t=0)$, the ODE (7.43) can be solved numerical for the flux ψ and thus also for current I using (7.42).

This model extends the models of the previous section to a variable impedance and thus allow to illustrate the inductive fault current limiting effect. This model still has limited applicability as it uses the expression for the solenoid.

7.6 Numerical Example

In this section we employ the model developed in the previous section to illustrate how a coil with a flux-variable impedance can work as a fault current limiter.

Figure 7.3: Rational Function Approximation of the B - H curve.

```

1 function [T,psi] = solve_rlcircuit(my_ctx)
2
3 %.. Compute initial condition taking phase shift into account..
4 Rpre = 5; Rpost = .1; R_init = Rpre+Rpost; Tfault = 1; Vmax = 28;
5 L_init = lookup_imped(0, my_ctx);
6 om = 2*pi*50;
7 X_init = sqrt(R_init^2 + om^2*L_init^2);
8 phase_shift = atan(om*R_init/L_init);
9 I_init = -Vmax/X_init*sin(phase_shift);
10 psi_init = L_init*I_init;
11
12 %.. Add DC component..
13 V_dc = -.4;
14 psi_dc = L_init*V_dc/R_init;
15
16 %.. Solve ODE for the magnetic flux..
17 Tend = 0.32;
18 options = odeset('RelTol',1e-12,'AbsTol',1e-12);
19 % options = [];
20 [T,psi] = ode45(@rlcircuit,[0 Tend],psi_init+psi_dc,options);
21
22 function dpsidt = rlcircuit(t,psi)
23
24     if (t<Tfault) Rline = Rpre+Rpost; else Rline = Rpost; end
25     Vline = V_dc + Vmax*sin(2*pi*50*t);
26     Limpd = lookup_imped(psi, my_ctx);
27     dpsidt = Vline - Rline/Limpd*psi;
28
29     end
30
31 end

1 function Limpd = lookup_imped(psi, my_ctx);
2

```

```
3  global Limpd
4
5  btopsi = my_ctx.btopsi;
6  murtoL = my_ctx.murtoL;
7  psi_dc = my_ctx.psi_dc;
8
9  %.. Find b..
10 b = psi/btopsi;
11
12 %.. Find relative permeability..
13 mur = bhcurve(b);
14
15 %.. Find inductance..
16 Limpd = murtoL*mur;
17
18 %.. Overwrite with an a-priori value
19 if (0)
20     Limpd = 1e-1;
21 end

1 function mur = bhcurve(b)
2
3  %..BH curve definition..
4  bha = 2.12e-4;
5  bhb = 7.358;
6  bhc = 1.18e6;
7
8  %.. Define mur-b2 curve
9  b2 = b.*b;
10 nur = bha + (1-bha)*b2.^bhb./(b2.^bhb+bhc);
11 mur = 1./nur;
12
13 %.. If desired, overwrite with linear material..
14 if (0)
15     mur = ones(size(b));
16 end
```


Chapter 8

FEM Computations of Inductance and Induced Voltage

8.1 Axi-Symmetrical Models

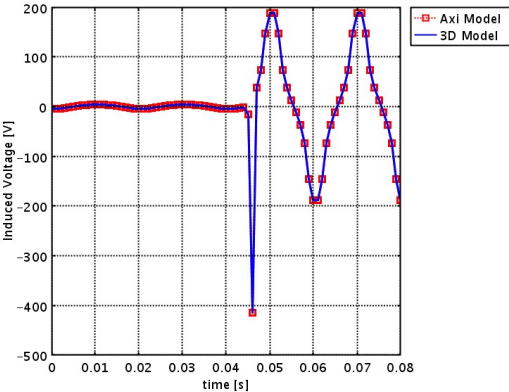
The following experimental data was provided to us by Johan Wolmarans.

1. Coil 1 (larger)
 - Inductance at 50Hz: 4.6mH
 - Turns: approximately 192, wound in 4 layers
 - Wire diameter: 1mm
 - Wound around 110mm diameter (55mm radius) pipe
 - Coil height: 60mm
2. Coil 2 (as used to measure the carbon fiber sleeve)
 - Inductance at 50Hz: 615uH
 - Turns: 81, wound in 1 layer
 - Wire diameter: 1mm
 - Wound around 118mm diameter (59mm radius) pipe
 - Coil height: 90mm

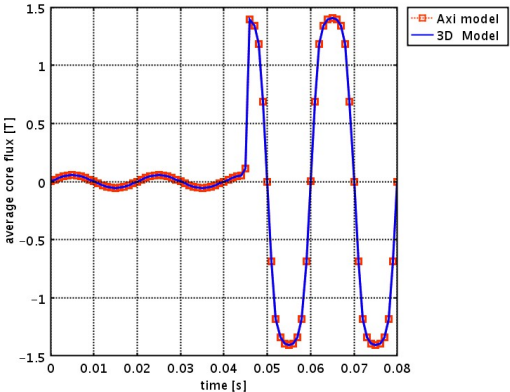
8.2 Three Dimensional Models

	L (mH)	pre fault (A)	post fault (A)
axi-symmetrical	3.39	4.55	16.58
cylindrical	3.24	4.59	16.87
cuboidal	4.51	4.51	14.00
cuboidal with open core	17.29	3.44	5.01

Table 8.1: Values of inductance, pre and post fault current in different configurations.

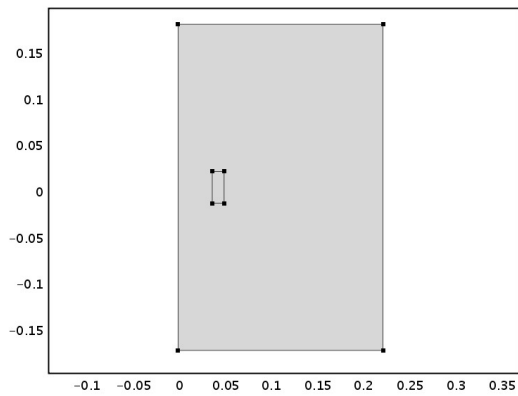


(a) Induced voltage

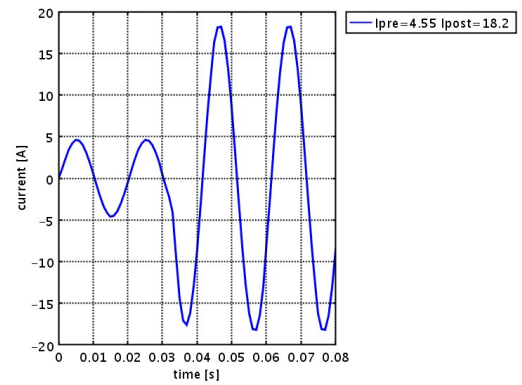


(b) Average magnetic flux

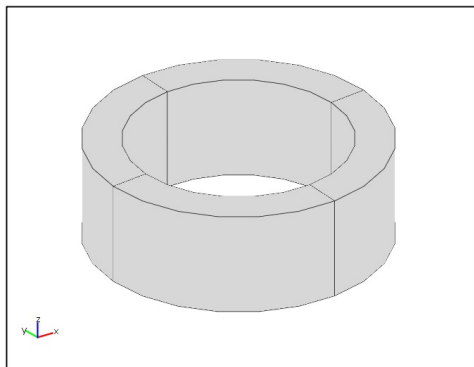
Figure 8.1: Axi-symmetrical and 3D computation of the induced voltage and magnetic flux.



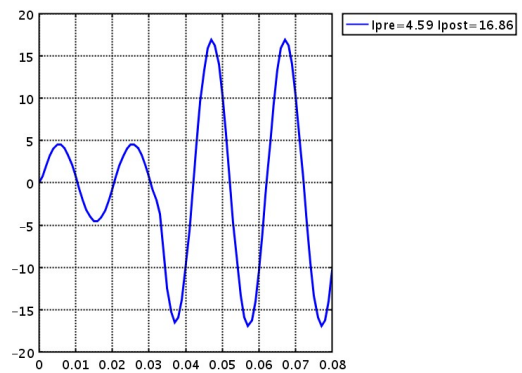
(a) Axi-symmetrical Model Geometry



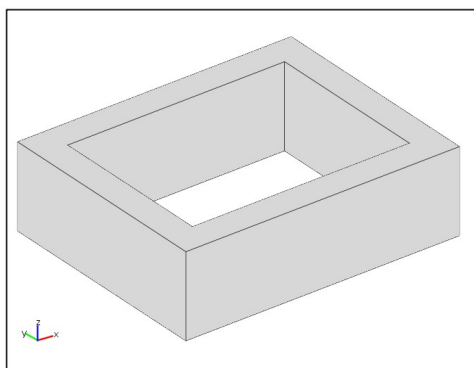
(b) Axi-symmetrical Model Current



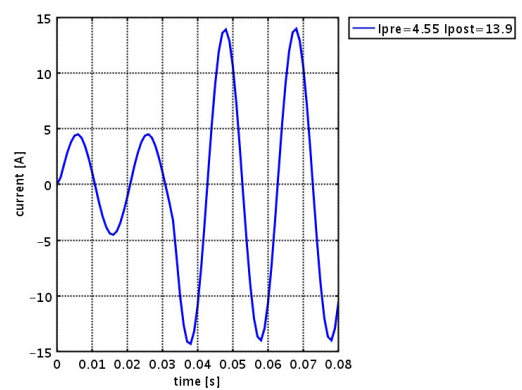
(c) Cylindrical Model Geometry



(d) Cylindrical Model Current



(e) Cuboidal Model Geometry



(f) Cuboidal Model Current

Figure 8.2: Different coil configurations and associated current waveforms.

Chapter 9

Two Dimensional FE Models of Inductive Fault Current Limiters

9.1 TO DO

1. in the first model

- choice of surface S motivated by desire to minimize influence of fringing and leakage flux
- investigate influence of space between coil and core
- investigate influence of gap in the core
- describe three stage process in solving the model
- include impedance computation after the second stage
- describe the setting of the initial guess in assembling the first jacobian (different from jacobian specified in femsolver!)

2. additional model

- open core model
- three legs model

Goals

- simulate RL-circuit without having to resort analytical model for the impedance
- compute the impedance of a given configuration in three different ways, using the analytical formula, the magnetic energy and the magnetic flux
- compute the current waveform using only the AC coil, the DC coil in two different polarities and with linear and non-linear core
- check the magnetic flux density in the core legs and verify using the BH-curve to what extent the DC coils brings the legs in saturation
- investigate to what extent an ODE model allows to simulate this configuration, eventually by first computing the impedance
- investigate to what extent the geometry of the coils affects the current waveforms
- document issues on time integration

9.2 Introduction

To do:

- give a definition of the induced voltage in 3D (using the winding function), and show how it simplifies to perpendicular and azimuthal current application

In these notes we develop a sequence of numerical models of increasing accuracy and complexity for the current in coils wound around ferromagnetic cores. We start by detailing analytical and semi-analytical models, build two-dimensional finite element methods and extend these into three dimensions. Modelling results for the current wave forms are compared with laboratory measurements on scale models of the devices under study. Initially we were motivated by comparing different configurations of so-called inductive fault current limiters. The study of these devices was presented at the Comsol Multiphysics Users Conference 2008 in Hannover (+ reference). The configurations we study are however representative for a wide range of other applications in AC/DC modelling such as electrical machines, transformers and actuators. We therefore decided to document the solution to different difficulties we encountered in the modelling in Comsol Multiphysics, hoping that you (the reader) might learn from it.

9.3 Inductive Fault Current Limiters

Wikipedia defines a fault Current Limiter (FCL) to be a device which limits the prospective fault current when a fault occurs. Different types exist. The fault current limiter we consider here is based on an inductor and consists of a ferromagnetic core and two coils (see Figure xxx). We will refer to the coils as the AC and DC coils. The AC coil carries the line current. The DC coil provides the magnetic field on which the working principle of the FCL under consideration is based. It's working principle is detailed in [?] and can be summarized as follows:

- **nominal regime:** a time-independent current in the DC coil bring the core in saturation. A sinusoidal line current flows through a wire represented by the AC winding. Parameters (ohmic resistance of the wire) are such that the left and right core leg do not desaturate, i.e., the impedance of the left and right core leg remain small.
- **occurrence of fault:** in case of fault, the drop in the ohmic resistance in the AC coil is compensated by the magnetically induced fields in the core, i.e., by the raise of the impedance of the coil. The particular construction of the FCL such that for $0 \leq t \leq T/2$ (where T denotes the period of the sinusoidal excitation of the AC coil) one of the core legs desaturates, causing the impedance (and thus the induced voltage) to raise and thus the current to be limited. During this period the other core leg remains in saturation, i.e., it does not contribute to the limiting process. During the period $T/2 \leq t \leq T$, the role of the left and right core leg are inverted, meaning that over the whole period T sufficient limiting is guaranteed.

9.4 Half Period Limiter

9.4.1 Geometry

In defining the geometry the core acts master and the coil as slaves. This corresponds to the fact that the coils are wound around the core.

1. the core:

(a) core variables

```
crwin = 12.5e-3; crwout = 37.5e-3; crwleg = crwout - crwin;
crhin = 39e-3; crhout = 63e-3;
rad = 3e-3;
```

(b) core:



Figure 9.1: Open-core configuration.

```
core = fillet(rect2(-crwout,crwout,-crhout, crhout), 'radii', rad) ...
        - rect2(crwin,crwin,-crhin,crhin);
```

2. flux integration lines:

(a) **left core leg:** line from (-crwout,0) to (-crwin,0)

```
fluxline1 = line1([-crwout,-crwin],[0,0]);
```

(b) **right core leg:** line from (crwin,0) to (crwout,0)

```
fluxline2 = line1([crwin,crwout],[0,0]);;
```

3. the AC coil:

(a) AC coil variables

```
accoilw = 10e-3; accoilh = 20e-3;
xspacer = 2e-3
accoilradin = crlegw/2+xspacer; accoilradout = accoilradin+accoilw;
coilxc = crwin+crwleg/2;
```

(b) AC coil:

```
accoil_right = rect2(accoilradin,accoilradout,-accoilh/2,accoilh/2);
accoil       = accoil_right+move(accoil_right,-2*accoilradin-accoilw,0);
accoil       = move(accoil,coilxc,0);
```

4. the DC coil:

(a) DC coil variables

```

dccoilh      = 10e-3; dccoilw = crwin/2;
dccoilradin  = (crhout-crhin)/2; dccoilradout = dccoilradin + dccoilh;
dccoilyc     = crhin+(crhout-crhin)/2;

```

(b) DC coil

```

dccoil_top   = rect2(-dccoilw/2,dccoilw/2,dccoilradin,dccoilradout);
dccoil       = dccoil_top + move(dccoil_top,0,-2*dccoilradin-dccoilh);
dccoil       = move(dccoil,0,dccoilyc);

```

5. the air:

(a) air variables

```

airh = 400e-3; airw = 400e-3

```

(b) air = rect2(-airh, airh, -airw, airw);

The 1D and 2D entities in the geometry are then combined using

```

clear c s
c.objs={fluxline1,fluxline2};
c.name={'fluxline1','fluxline2'};
c.tags={'g5','g6'};

s.objs={air,accoil,dccoil,core};
s.name={'air1','accoil','dccoil','core'};
s.tags={'g1','g2','g3','g4'};

fem.draw=struct('c',c,'s',s);
fem.geom=geomcsg(fem);

```

9.4.2 Constants, Functions and Subdomain and Global Expressions**Constants**

Note that a fill-factor in the coils is **not** used as the expression for the induced voltage in scaling invariant for the induced voltage.

Functions Functions are used to define the different BH-curves.

Global expressions The flux variables and their derivatives are included to check the model. They are not used in the computation as such. Flux variables are used to verify whether or not the core legs are in saturation. The flux

Electrical constants	
ω	$2 \pi 50$
Vmax	28
Rpre	4.0
Rpost	0.1
Tfault	45e-3
Tsmooth	1e-3
Core	
lz (Length in z-direction)	25e-3
fcrwleg	crwleg
crcross (Core leg cross-section)	fcrwleg*lz
AC coil	
acNt (Number of turns)	200
accross (Cross-section)	accoilw*accoilh
Iac (Current value)	5
DC coil	
dcNt (Number of turns)	250
dccross (Cross-section)	dccoilw*dccoilh
Idc (Current value)	10
BH curve data	
linmurfe	1000
bha	2.12e-4
bhb	7.358
bhc	1.18e6
C ₁	.25
C ₂	.06

Table 9.1: Constants Used

derivative variables are used to check the induced voltage.

$$Vline = Vmax \sin(\omega t) \quad (9.1)$$

$$Rline = Rpre - (Rpre - Rpost) * flc2hs(t - Tfault, Tsmooth) \quad (9.2)$$

$$Vind1 = -\text{sign}(Jz) * acNt * lz / accross * Eint1 \quad (9.3)$$

$$Vind2 = -\text{sign}(Jz) * acNt * lz / accross * Eint2 \quad (9.4)$$

$$Vind = Vind1 + Vind2 \quad (9.5)$$

$$Bavrg1 = Bint1 / crwleg \quad (9.6)$$

$$Bavrg2 = Bint2 / crwleg \quad (9.7)$$

$$fluxt1 = -acNt * lz * Btint1 \quad (9.8)$$

$$fluxt2 = -acNt * lz * Btint2 \quad (9.9)$$

9.4.3 Integration Coupling Variables

We keep two variables for the induced voltage in order to be able to monitor them separately. Subdomain integration coupling variables for the induced voltage

$$Eint1 = \int_{accoil1} E_z d\Omega = \int_{accoil1} \frac{\partial A_z}{\partial t} d\Omega \quad (9.10)$$

$$Eint2 = \int_{accoil2} E_z d\Omega = \int_{accoil2} \frac{\partial A_z}{\partial t} d\Omega \quad (9.11)$$

and boundary integration coupling variables for the average flux and the time-derivative of the flux

$$Bint1 = \int_{fluxline1} B_y dl = \int_{fluxline1} -\frac{\partial A_z}{\partial x} dl \quad (9.12)$$

$$Bint2 = \int_{fluxline2} B_y dl = \int_{fluxline2} -\frac{\partial A_z}{\partial x} dl \quad (9.13)$$

$$Btint1 = \frac{d}{dt} \int_{fluxline1} B_y dl = \int_{fluxline1} -\frac{\partial^2 A_z}{\partial x \partial t} dl \quad (9.14)$$

$$Btint2 = \frac{d}{dt} \int_{fluxline2} B_y dl = \int_{fluxline2} -\frac{\partial^2 A_z}{\partial x \partial t} dl \quad (9.15)$$

where the minus sign in the expressions with index two take the direction of the current into account.

9.4.4 Application mode, subdomain and boundary settings

The magnetic field is modeled by a partial differential equation for the z -component of the magnetic vector potential A_z (perpendicular current model) satisfying the following equation

$$\sigma \frac{\partial A_z}{\partial t} + \frac{\partial}{\partial x} (\nu_0 \nu_r(B) \frac{\partial A_z}{\partial x}) + \frac{\partial}{\partial y} (\nu_0 \nu_r(B) \frac{\partial A_z}{\partial y}) = J_z(x, y, t) \quad (9.16)$$

where $\sigma = 0$ everywhere on Ω , supplied with boundary conditions. All time-dependency is thus in the current source! We do solve this equation with a time-stepping procedure as we need the derivative $\frac{\partial A_z}{\partial t}$ in defining the induced voltage.

- material characteristics:
 - ferromagnetic core: μ_r through BH-curve
 - coils and air: $\mu_r = 1$

- current excitation
 - DC coil: constant current density equal to $J_{z,dc} = \pm \frac{I_{dc,tot}}{S_{dc}} = \pm dcNt \frac{Idc}{d_{cross}}$
 - AC coil: voltage driven by a sinusoidal voltage source V_{line} through the circuit relation given below. The variable I_{tot} is to be computed such that $J_{z,ac} = \pm \frac{I_{ac,tot}}{accross} = \pm acNt \frac{I_{tot}}{accross}$

Different Application Modes In different application modes we subsequently solve for

- the impedance using three different models
- the initial guess for the transient simulation
- the non-linear transient simulation including the fault

9.4.5 ODE Settings

The current in the AC coil is modeled by a circuit relation (an ODE) for the variable I_{tot}

$$V_{tot} = V_{res} + V_{ind} \quad (9.17)$$

$$= RI_{tot} + V_{ind1} + V_{ind2} \quad (9.18)$$

9.4.6 Numerical Results

Discuss that

- this configuration is not able to limit the during during both periods.

9.5 Open-Core Configuration

1. geometry of the AC coil changes

9.6 Three-Leg Configuration

1. new geometry
2. DC coils opposite polarity, AC coils different polarity
3. in the computation of the inductance only *only* AC coil needs to be taken into account
4. new integration coupling variables
5. new ODE setting



Figure 9.2: Three legged core configuration.

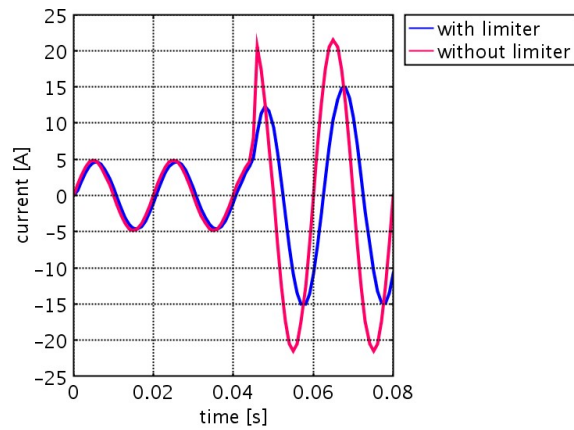
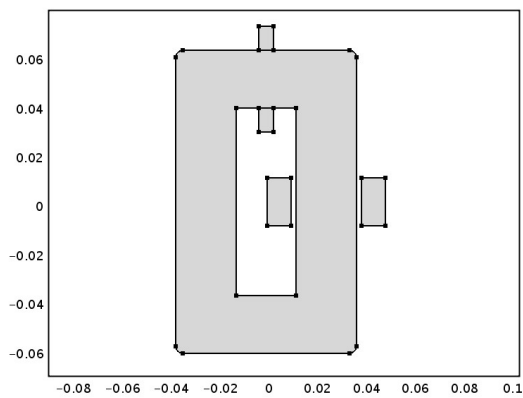
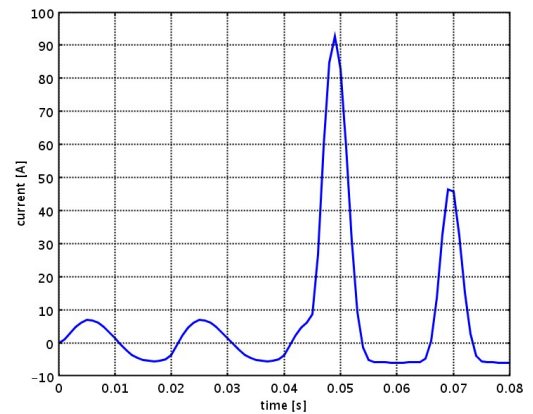


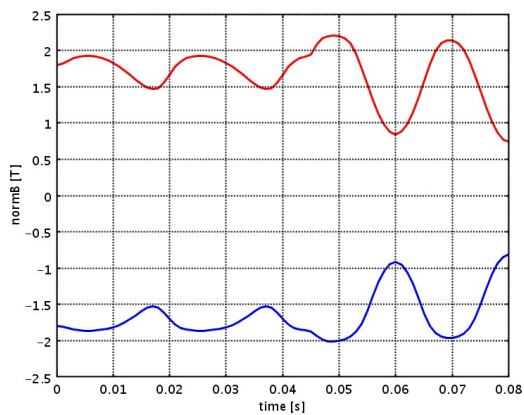
Figure 9.3: Current with and without limiter.



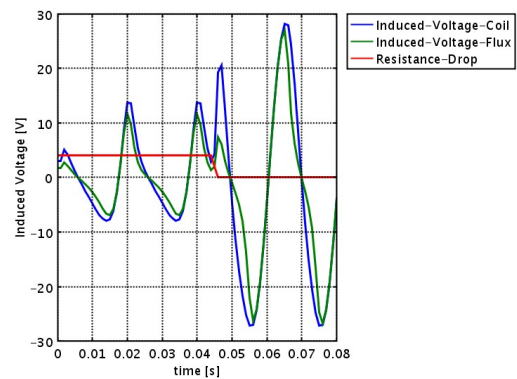
(a) Geometry



(b) Computed line current



(c) Flux in left and right core leg



(d) Induced Voltage

Figure 9.4: Numerical results for the O-shaped core configuration.

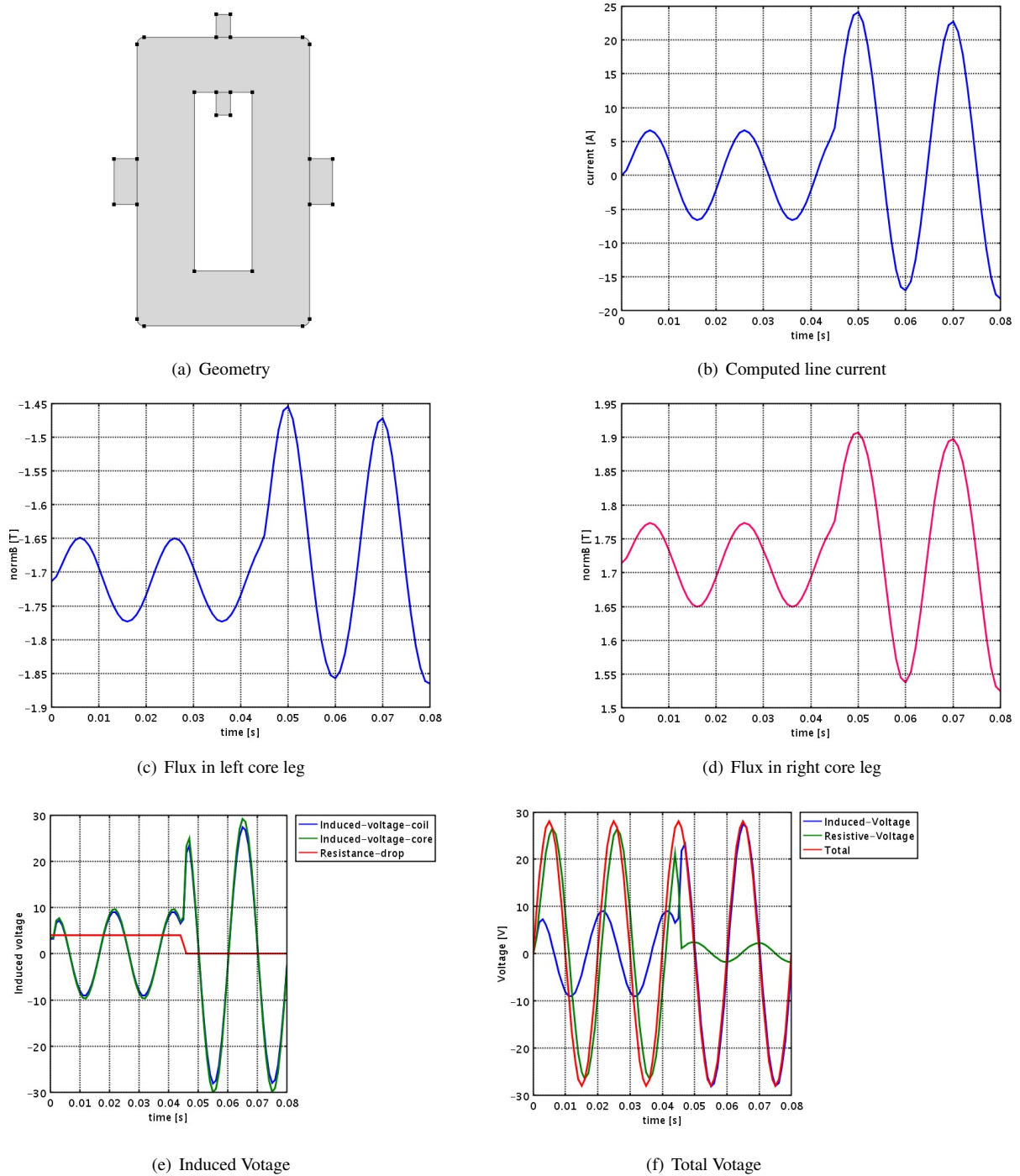


Figure 9.5: Numerical results for the open-core configuration.

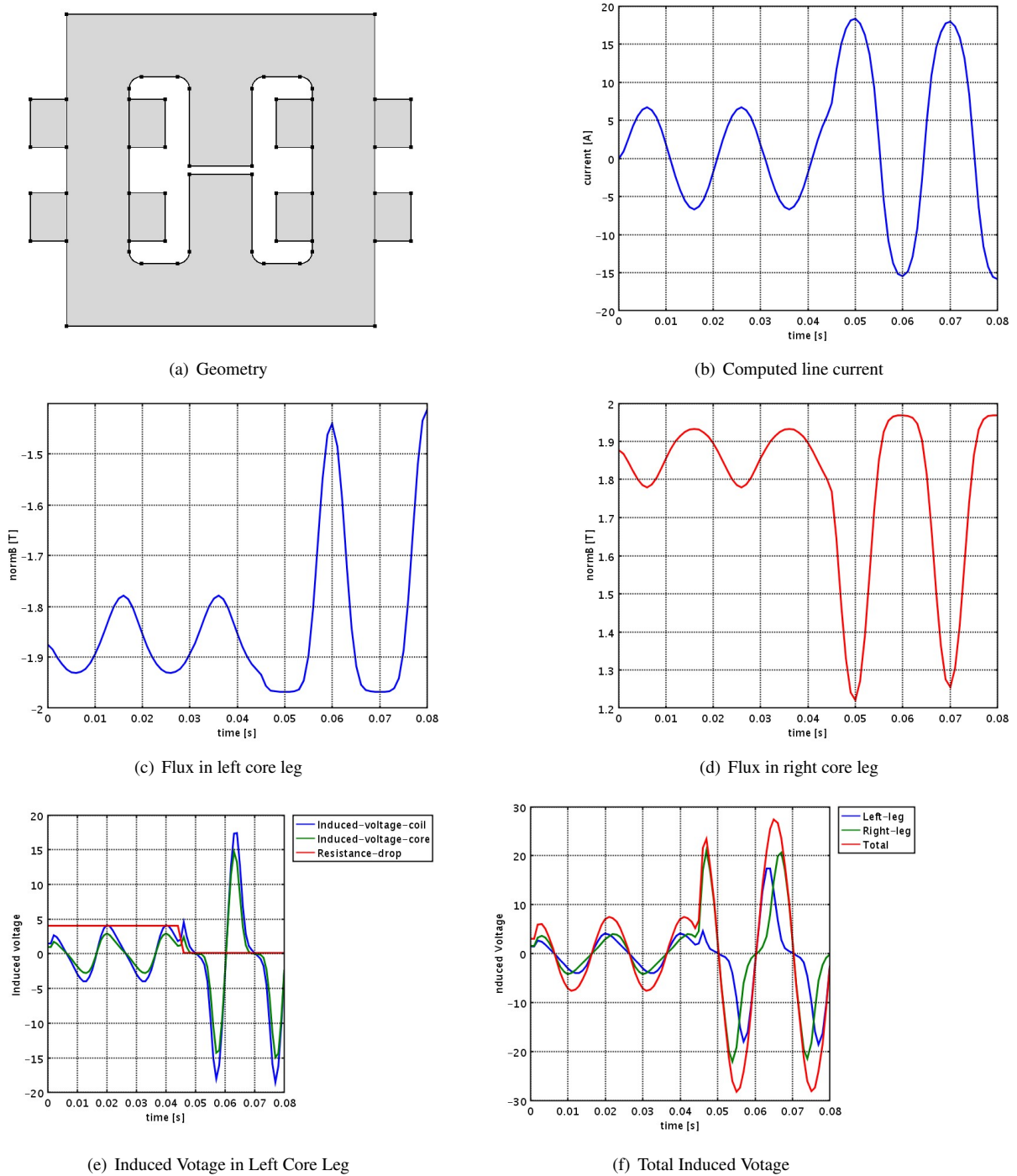


Figure 9.6: Numerical results for the three-legs configuration.

Chapter 10

Three Dimensional FE Models of Inductive Fault Current Limiters

To do

- add references to De Gersem and Dular on the field circuit coupling

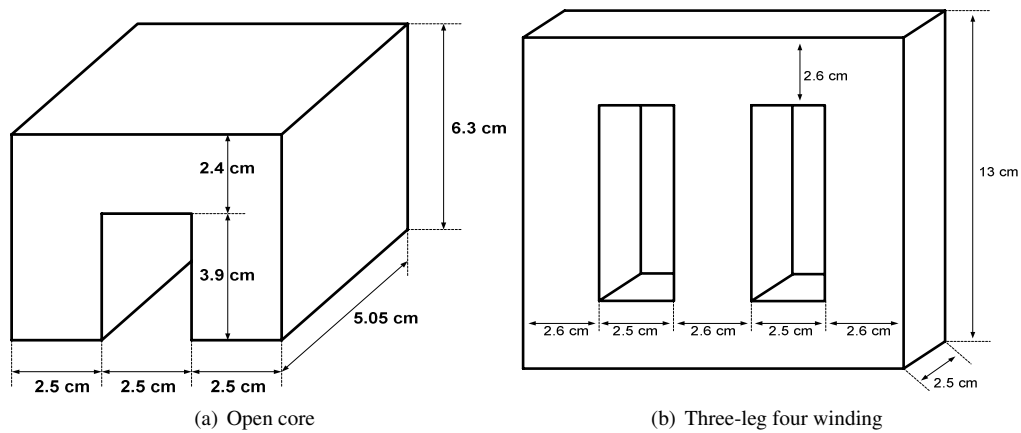


Figure 10.1: Geometries studied

10.1 Open-Core Configuration

10.1.1 Geometry

In defining the geometry, the core acts as *master*, while the DC and AC coil act as slave. The geometry will consist of the following four parts:

1. **the core:** build by extruding a working plane in the yz -plane in the x -direction. There will be a relation between the depth and width of the core leg.

(a) core variables

```
crlegw = ;  
crwin = ; crwout = crwin + crlegw;
```

```
crhout = ; crhin = ;
crd = ;
```

(b) core working plane:

```
core_plane = fillet(rect2(-crwout,crwout,-crhout, crhout), 'rad', rad) ...
              - fillet(rect2(crwin,crwin,-crhin,crhin), 'rad', rad);
```

(c) core extrusion

```
set working plane at x = 0
core = extrude(core_plane, 'distance', 2*crd);
```

2. **flux integration surfaces:**

3. **the generic coil:** build by extruding a working plane in the xy -plane in the z -direction

(a) generic coil variables

```
coilw = ; coilh = ;
yspacer = ; zspacer = ;
coilradin = crlegw/2+yspacer; coilradout = coilradin+coilw;
coilyc = crwin+crwleg/2; coilzc= coilh/2 + zspacer;
```

(b) coil working plane:

```
coil_plane = circ2(coilradout) - circ2(coilradin);
```

(c) coil extrusion

```
set working plane at z = 0
coil = extrude(coil_plane, 'distance', coilh)
```

4. **the DC coil:** by moving the generic coil in positive y -direction and in positive z -direction

(a) DC coil variable

```
dccoilzc= coilh/2 + zspacer;
```

(b) dccoil = move(coil,0,coilyc,dccoilzc);

5. **the AC coil:** by moving the generic coil in positive y -direction and in negative z -direction

(a) AC coil variable

```
accoilzc= -coilh/2 - zspacer;
```

(b) accoil = move(coil,0,coilyc,accoilzc);

6. **the air:** build using the `block3` command

For the ease of modification of this geometry we will work with a full model.

10.1.2 Meshing

Currently the meshing happens fully automatically, excepts for the option `hauto` used in `meshinit`. Due to this automation, difficulties may occur in case the space between the coils and the core leg is too small. This issue will have to be dealt with in the future.

10.1.3 Constants, Functions and Subdomain and Global Expressions

Constants

Note that a fill-factor in the coils is **not** used

Electrical constants	
ω	$2 \pi 50$
DC coil	
Number of turns Cross-section Current value	
AC coil	
Number of turns Cross-section BH curve data	
a	2.12e-4
b	7.358
c	1.18e6
C ₁	.25
C ₂	.06

Table 10.1: Constants Used

Functions

Here we define the BH curves and the winding functions.

Subdomain expressions

Here we define the densities for the induced voltage

Global expressions

Here we define the electrical excitation and the induced voltage.

10.1.4 Application modes

We solve for both the vector and scalar potential. The scalar potential is used to avoid that during time integration components in the null space of the curl-curl operator are introduced.

10.1.5 Integration coupling variables

Here we integrate the induced voltage density to obtain the total induced voltage.

10.1.6 Definition of the ODE

The sum of resistive and induced voltage is at all times equal to the total applied voltage.

10.1.7 Solution process

10.1.8 Post processing

10.2 Different solution modes

10.2.1 Linear core

10.2.2 Non-linear core

Define the different stages.

Bibliography

- [1] J. C. Maxwell. *A Treatise on Electricity and Magnetism*. Reprint in Clarendon Press, 1891.
- [2] Q. Quarteroni and A. Valli. *Domain Decomposition Methods for Partial Differential Equations*. Oxford Science Publications, 1999.
- [3] A. Sommerfeld. *Electrodynamics*. Academic Press, New York, 1952.